AN UNSTABLE ARCH MODEL OF A SOLAR FLARE

DANIEL S. SPICER

E. O. Hulburt Center for Space Research,
U.S. Naval Research Laboratory, Washington, D.C. 20546, U.S.A.

and

Institute for Fluid Dynamics and Applied Mathematics,
University of Maryland, College Park, Md., 20742, U.S.A.

(Received 22 June, 1976; in revised form 28 January, 1977)

Abstract. The theoretical consequences of assuming that a current flows along flaring arches consistent with a twist in the field lines of these arches are examined. It is found that a sequence of magneto-hydrodynamic (MHD) and resistive MHD instabilities driven by the assumed current (which we refer to as the toroidal current) can naturally explain most manifestations of a solar flare.

The principal flare instability in the proposed model is the resistive kink (or tearing mode in arch geometry) which plays the role of thermalizing some of the field energy in the arch and generating X-configured neutral points needed for particle acceleration. The difference between thermal and nonthermal flares is elucidated and explained, in part, by amplitude-dependent instabilities, generally referred to as overlapping resonances. We show that the criteria for the generation of flare shocks strongly depend on the magnitude and gradient steepness of the toroidal current, which also are found to determine the volume and rate of energy release. The resulting model is in excellent agreement with present observations and has successfully predicted several flare phenomena.

1. Introduction

The solar flare, probably the most dramatic event in the solar atmosphere, has long been an enigma to the observer observing it and to the theorist trying to explain it. The principal reason for this lack of progress is simply that the flare theorist has tended to concentrate on mechanisms that can convert stored energy, such as magnetic energy, into the energy of the solar flare, instead of dealing with a specific model with its attendant detailed field geometry. In his quest for such mechanisms the theorist has often shown little regard for the observations, and a specific flare model has never really been elucidated, with the possible exception of Sturrock's (1966, 1968, 1972, 1974) and Syrovatskii (1966). However recently (Vaiana and Gioconni, 1968; Widing and Purcell, 1969; Widing, 1973; Spicer *et al.*, 1974; Widing and Cheng, 1975; Widing, 1974; Widing and Cheng, 1975) the data have indicated that the principal magnetic topology of a flare is that of an arch and not that of a current sheet as, e.g., is assumed by Sturrock and is currently in the theoretical vogue. Hence it is the purpose of this paper to deal with the observed flare geometry and to show that all the theoretical ideas developed in sheet models have not gone to nought but can, in general, be reapplied in arch geometry or similar geometry with some rather pleasing results.

For a flare model to be reasonably complete it should be able to describe the basic sequence of events that leads to a flare, its evolution, and finally its

Solar Physics **53** (1977) 305–345.

secondary effects. Further we should accept the premise that for a model to be useful it must not only explain what is known but should also predict new effects and thus be capable of development. In the model to be presented here we cannot accurately calculate the energy distribution of the accelerated particles, nor can we explain rigorously the origin of the currents necessary to explain the flare within the context of the flare model. However we can explain most of the well-established observations and make some new predictions. Phenomena that require a detailed theoretical prediction are not discussed at this stage, simply because observations of the relevant parameters necessary for accurate calculation do not have sufficient spatial or temporal resolution to make any detailed treatment meaningful. As new detailed observations, e.g., the temperature and density structure of an arch become available, we should then be able to make more accurate predictions; e.g., one could develop an overall computer code for the model which could evolve in sophistication as more detailed input becomes available.

This paper is organized as follows: First, in Section 2, we briefly review the recently obtained Skylab data while commenting on how these data affect older flare models. The principal observation is that the magnetic topology of the flare volume is that of an arch or similar configuration, which may have a complicated structure, e.g., currents and return currents.

In Sections 3, 4, and 5 we develop the flare model. In Section 3 we discuss the location of the arch in the solar atmosphere which is necessary to explain the observations. We then proceed to discuss the various types of flares which we expect can be accommodated within the model, e.g., impulsive or those with a gradual rise and fall. We then show that the resistivity need not be anomalous to explain the flares observed by Skylab, although if the resistivity were to become anomalous, the required volume of energy release would be very small, $\approx 10^{20}$ cm^3. Further, a discussion of mechanisms that can form impulsive electromagnetic bursts and shocks is given in Section 4. Also, mechanisms for particle escape from the arch are pointed out. It is then noted that the model predicts all flares should be impulsive in part, the difference then between thermal and nonthermal flares being only an experimental sensitivity problem. Possible mechanisms that can trigger the resistive kink mode are then discussed under precursors. Here, for example, more intense coronal hearing by waves and shock waves from other flares are found to act as possible flare percursors.

We conclude, in Sections 6 and 7, with a discussion of the expected flare phenomenology. A number of predictions concerning preflare behavior and arch behavior during the flare are made. In addition we note that any arch which carries a current should be subject to the sequences of instabilities discussed and that this point may explain the postflare loop phenomenon, X-ray bright points, and the slow rise and fall events recently reported (Sheeley, 1976).

Before proceeding, we note that probably the most appealing aspect of this model is its simplicity. That is, the model requires only a current-carrying arch or

similar sheared structure, which, as Skylab has aptly proved, appears to be the dominant magnetic structure within an active region. Thus it is hoped that whether the model presented here is correct or incorrect, it will serve to point out that current sheet models, the vogue for nearly 20 years, are not the only answer.

2. Recent Flare Observational Results

Probably the most significant observational result for flares of the last decade has been the apparent determination of the magnetic topology of the flare. With this knowledge one can radically narrow the number of possible mechanisms that can occur in the topology once the topology is determined. Skylab ATM observers have reported (Widing, 1974a, b; Widing and Cheng, 1975; Cheng and Widing, 1975; Spicer *et al.*, 1974; Petrasso *et al.*, 1975; Vorphal *et al.*, 1975; Gibson, 1977; Kahler *et al.*, 1975; Brueckner, 1975) that the basic magnetic configuration of the solar flare appears to be that of an arch. Figure 1 illustrates the basic conclusions concerning the geometric structure of the flare plasma. One should

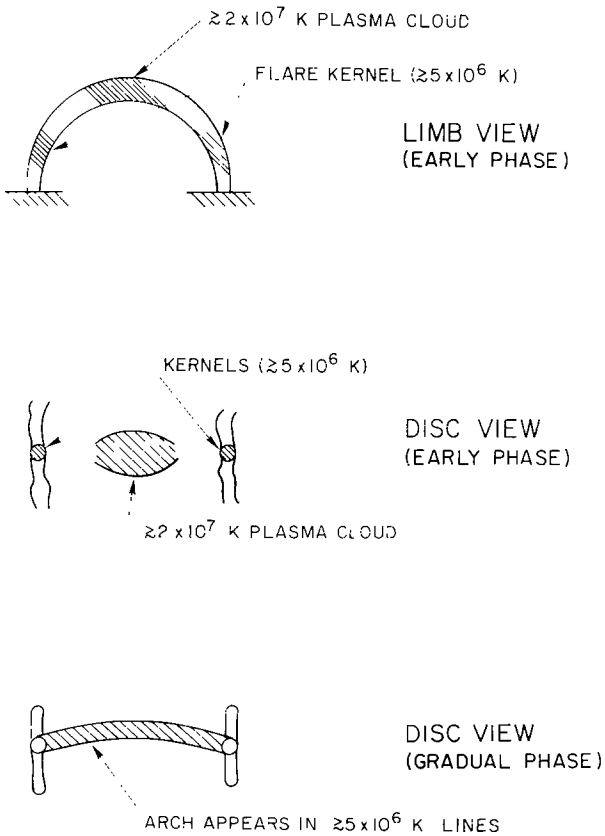

Fig. 1. Observed flare geometry.

note:

– The primary flare ingredient appears to be an archlike structure;

– A localized hot plasma cloud ($\geq 20 \times 10^6$ K and $\geq 10^{11}$ particles cm^{-3}) exists near or at the apex of the arch during the early flash phase, this cloud is elongated along the arch;

– The flare kernels have their origins at the ends (feet) of the arch, and these kernels are located in the double ribbons of the flare;

– The arch is oblique to the neutral line (the line along which the measured component of B normal to the solar surfaces vanishes) and each flare ribbon lies on each side of the neutral line;

– As the plasma cools, the arch becomes very apparent in the cooler lines ($\approx 2 \times 10^6$ K);

– The feet of arch clearly originate in bipolar regions and connect differing polarities;

– The small volume of the hot plasma core is indicative of well-localized heating, and the energy appears to be released in situ in this core;

– The arch exhibits great stability during most of the flare;

– Many of the observed flares appears to be thermal flares and show little dynamic behavior;

– Evidence has been found that the flare may undergo repeated heatings, occurring in differing arches (Widing and Dere, 1977);

– Evidence supports the assumption that neighboring arches may flare due to shock disturbances generated by the initial flare (Vorpahl, 1976);

– Recent evidence, albeit weak evidence, suggests that some arches kink, but it is not clear whether all the kinking arches are the flare arches of higher lying arches (Gibson, 1977; Cheng, 1976);

– The rise time, decay time, and rate of increase of soft X-ray emission tends to increase with flare volume (Gibson, 1977);

– The volume of in situ intense heating was of about 2 cubic arcseconds, corresponding to volume scales of 2.7×10^{24} cm^3.

Preflare observations (Petrasso *et al.*, 1975; Brueckner, 1975; Gibson, 1977; Patterson *et al.*, 1976) have found:

– The arches are observed to brighten, sometimes gradually (hours) and sometimes quickly (about 10 min), prior to flaring;

– Line spectra from the transition zone show that the transition zone is undergoing strong agitation;

– Subflares appear as arches and show strong agitation in transition zone lines;

– The arches are observed to exist prior to flaring.

These observations are in complete contradiction to all existing flare models except possibly the 'current interruption model' (Alfvén and Carlquist, 1967). This model however has been criticized theoretically (Smith and Priest, 1972). Although all the criticisms made are not correct (Spicer, 1974), interruption of the bulk current in an arch, by anomalous processes or otherwise, is highly unlikely (a

detailed discussion will be published elsewhere). With these results and their obvious inconsistency with present flare theories, there is strong motivation to look elsewhere for an explanation of a flare.

3. Basic Flare Mechanism

Our purpose here is to establish whether a current-carrying arch in the solar atmosphere, subject to MHD and resistive MHD modes can release the explosive energy (typically of the order 10^{28} erg s^{-1} for a small flare) associated with a flare. We establish this by determining the location of the current-carrying arches that we expect will cause the classically defined flare, i.e., those flares that result in intense chromospheric heating. This allows us to assume reasonable magnitudes for various parameters, such as poloidal field strengths in the arches. With the location of these arches determined, we then show that the occurrence of MHD and resistive MHD instabilities in arches can explain the energy release of a flare.

In what follows we will apply rather freely various mechanisms in subsequent sections, which have neither been collected together in a review or text nor been discussed adequately in the astrophysical literature for present purposes. For this reason the reader should consult Spicer (1976a) for a more thorough presentation of all the mechanisms used here.* (Figure 2 illustrates the sequence of mechanisms, which will lead to a flare in this model.)

The principal geometry of the flare model to be proposed is that of a semitoroidal magnetic arch illustrated in Figure 3, along which a toroidal current J_T is assumed to flow in some as yet unspecified manner and driven by as yet unknown mechanisms. The assumption that a toroidal current flows along the main toroidal field of the arch implies that we are in reality considering a diffuse pinch bent into a half torus. Thus it follows that we will be interested in the stability of such a configuration. As we will soon see, such a diffuse pinch will be subject to MHD kink modes and resistive kink modes; the former differing from the latter in that the former strictly conserves magnetic flux whereas the latter permits reconnection within the arch. However both kink modes are driven by the magnetic field energy stored in the poloidal field B_p generated by the toroidal current, and one can excite the other.

As will become evident during our discussion, MHD and resistive MHD stability of the arch will be determined by the degree of magnetic shear in the arch. However the stability criteria obtained depend critically on the quantity $\mathbf{k} \cdot \mathbf{B}$ and where it vanishes, $\mathbf{k}$ being the wave-number vector of the perturbation and $\mathbf{B}$ the magnetic field. Since the stability in both the MHD and resistive cases was analyzed assuming cylindrical symmetry, which an arch clearly does not have, it was necessary to show that the stability criteria obtained using cylindrical

* Copies of this report can be obtained directly from the author by request.

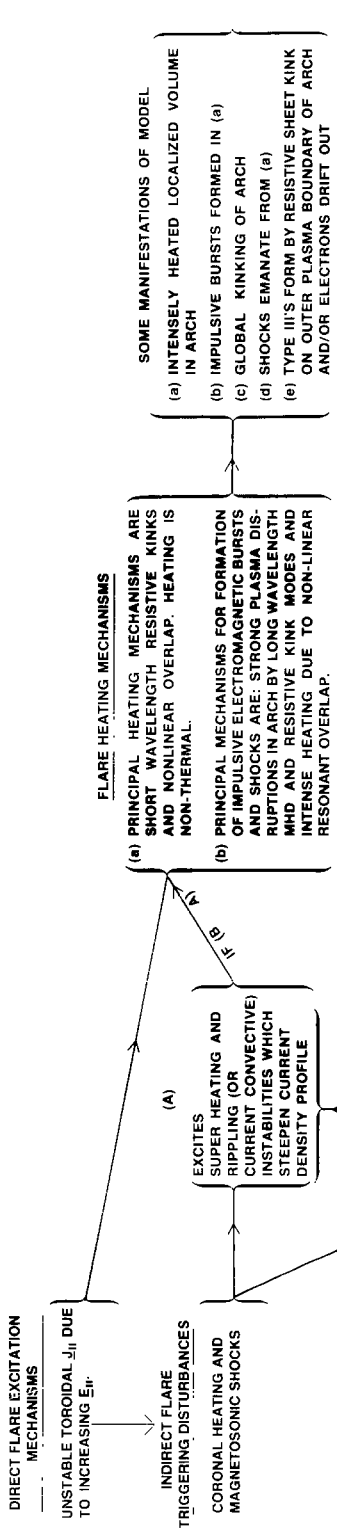

Fig. 2. Flow chart of the arch flare model being proposed.

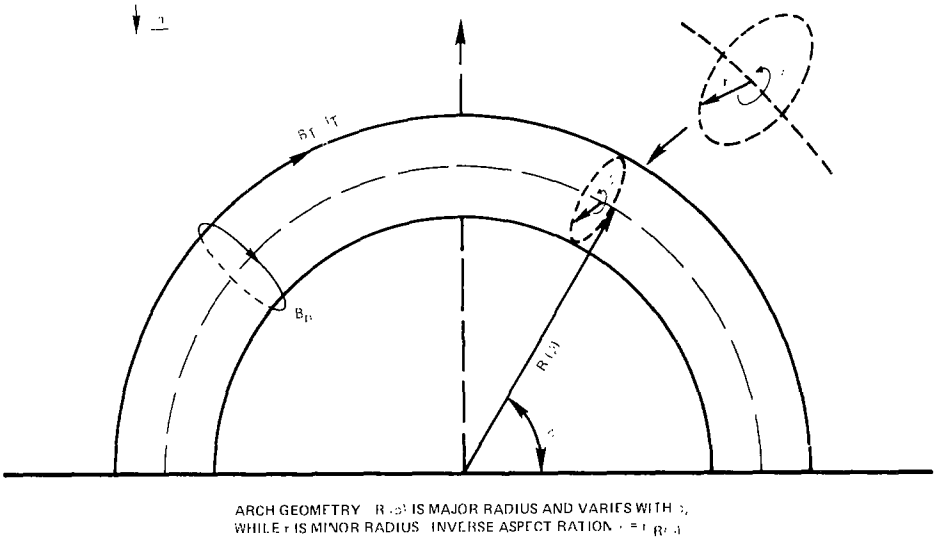

Fig. 3. Principal geometry of arch flare model being proposed.

symmetry is valid in more complex geometries such as the arch. This proof can be found in Spicer (1976a).

Further, during our discussion we will note that the increase in complexity of the arch can give rise to complex nonlinear phenomena, which may prove useful in explaining certain behavior of the solar flare in the context of this model. These phenomena arise because of the complex distortion of magnetic surfaces due to the arch curvature and the distortion of magnetic surfaces generated by the flux-conserving MHD kink modes. This follows because the resistive kink mode or tearing mode can be treated as a symmetry-breaking mechanism, since it does not conserve flux. Indeed the resistive kink mode can result in neighboring surfaces nonlinearly interacting with one another, thereby causing a sudden and dramatic increase in reconnection, over and above that caused by one surface reconnecting. Since this nonlinear phenomenon has a threshold it must cross before occurring, we will argue that it may be one possible explanation for the nonthermal electromagnetic bursts associated with flares. A detailed discussion of these mechanisms can be found in Spicer (1976a).

Because the location where $\mathbf{k} \cdot \mathbf{B}$ vanishes determines in part the stability of the arch, we require a knowledge of mechanisms that can steepen the radial profile of the toroidal current. Further, we require a knowledge of mechanisms that may prevent this current-density steepening. This is important, because the arches are observed to exist prior to flaring; i.e., they were not always arches emerging from the photosphere. Hence we need to know those mechanisms that can lead to instability and how they manifest themselves.

3.1. Location of arches that cause flares

To determine precisely the location of arches that flare is difficult without a substantial improvement in our empirical knowledge of the physical conditions within these arches. However we can heuristically determine where we expect the arches that do flare to exist. Hence what follows should be considered in part as predictions of the model.

We begin by recognizing that the locations of a particular kind of flare (e.g., impulsive rise versus gradual rise) is undoubtedly related to the rate of energy released, which in turn is determined by the magnitudes and gradients of quantities like the magnetic field and density, which are in turn determined by the arches' size and location. Keeping this in mind, one can represent the rate at which magnetic energy is thermalized by the tearing mode by

$$\frac{d\varepsilon}{dt} \approx \frac{\gamma B_p^2 \Delta V}{4\pi}, \tag{3.1}$$

where ΔV is the incremental volume along the arch in which the tearing mode occurs. The poloidal component of **B** occurs in Equation (3.1) because it is the principal component of field dissipated. Since γ and B_p are in general functions of position in the arch, $d\varepsilon/dt$ will differ at different locations along the arch. Further, since γ and B_p are strongly influenced by both the magnitudes and gradients of various parameters, we should expect $\gamma B_p^2/4\pi$ to be greatest where the magnitudes and gradients of these parameters maximize it. Hence we should expect the *location of instability to appear well localized within the arch;* i.e., *the incremental volume ΔV should be such that $\Delta V/V \ll 1$, where V is the total arch volume.* This is what is observed (Widing and Cheng, 1975; Cheng and Widing, 1975). Indeed, since observationally ΔV is small, $\gamma B_p^2/4\pi$ must necessarily be large, which implies steep gradients and large B_p, which in *turn clearly implies the arches must exist low in the solar atmosphere if they are to explain solar flares.*

If we were to require the bulk current to be electrostatically unstable at flare onset, we again would be forced to require the arches to be low lying, since the field gradients would then have to be of the order of a skin depth, if the current is to be electrostatically unstable.

An alternate means of determining which arches will flare is to ask about the global stability of the arch. As discussed in Section 2, arches are observed to exist prior to their flaring and appear stable. If they are to be MHD stable, they must be stable against the global kink mode prior to flaring. This requires the safety factor q, to satisfy $q \gg 1$ at every point in the arch. To see this, we note that by flux conservation $B_{T_0} r_0^2 = \text{constant}$ and $B_{p_0} \approx 2I/cr_0$, where I is the total toroidal current and assumed here to be constant. Hence, since $q = \pi r_0 B_{T_0}/B_{p_0} L$, we find q approximately independent of position along the current path. (In Spicer, 1976a we examine this point more critically.) Two things are clearly represented in $q \gg 1$: the larger is $2\pi r/L$, the greater is q, and the larger is the ratio B_t/B_p, the

greater is q. These requirements however can be satisfied in small or large arches for suitable parameter regions. Thus, to continue our argument, we must turn again to flare energy requirements.

Since B_p must be relatively large to explain the energy release from an arch, we must also have B_T large for a fixed $2\pi r/L$ if q is to remain above 1. However, to obtain a large B_T requires that we descend in altitude, since B_T increases with decreasing altitude. But in so doing L will usually decrease, causing $2\pi r/L$ to increase. These arguments imply that for an arch to be kink stable prior to flaring and then to release enough energy to explain a flare, it must have a relatively low altitude.

These arguments can be supplemented by noting the stabilizing effect of the conducting ends on the arch and demanding the arch be stable against G modes. As shown by Solovev (1971), a sufficient condition for stability for a cylindrical diffuse pinch attached to conducting ends is

$$\frac{j_T L}{\pi c B_t} < 1, \tag{3.2}$$

and the necessary condition is

$$\frac{j_T^2 r L}{8\pi B_T^2 c^2} < 1. \tag{3.3}$$

Both conditions require B_T to be large and L to be small. Further, the arch will be stable against resistive G quasi-modes if the β of the arch satisfies $\beta < \beta_{\text{critical}}$, where

$$\beta_{\text{critical}} = \frac{r c_s^2}{g\pi L^2}. \tag{3.4}$$

This can be cast in the form

$$\frac{L^2 \pi g \beta}{r c_s^2} < 1, \tag{3.5}$$

which again implies L must be small and B_T must be large. We can then predict that for an unstable arch to act as a flare and to release the appropriate amount of energy in the required amount of time, it must be low lying with a small length.

So far we have demanded the arch be MHD stable. Alternately we can demand that the bulk toroidal current density j_T be electrostatically stable prior to flare onset. A sufficient condition for the bulk current to be electrostatically stable is that the drift velocity V_d be less than some critical thermal velocity. Since the Buneman instability is the least likely current-driven instability, we impose the condition that the bulk current be stable against the electrostatic ion cyclotron and ion sound modes. Using Amperes' law, $j_T = n e v_d$, and $v_d \ll c_s$, we require

$$n \gg 2.29 \times 10^5 \frac{j_T}{\sqrt{T_e}} \tag{3.6}$$

within the arch, if the current is to remain electrostatically stable. Since, the larger is n, the greater is the conductive and radiative cooling, we should expect T_e to be low in the stable low-lying arch. Further, since observationally $n \approx 10^{11}$ to 10^{12} cm^{-3} in the flaring arches, and the smallest observed temperature in the solar atmosphere is 6000 K, we should expect j_T to satisfy $j_T \ll 10^8$ statampères cm^{-2} in the arch prior to its flaring. As we shall see, $j_T > 10^7$ statampères cm^{-2} is of the order required to explain the energy release of the flare. We can then forsee requiring a preflare steeping of current density within the arch.

To summarize, *we have predicted that the arches prior to flaring are low lying, with a small length, high density and probably a low temperature,* at least in the arch core, i.e., $r \approx 0$. Later, after we discuss flare energy requirements, we will estimate the length and height of an arch for the parameters to be adopted.

From the preceding discussion one should expect various classes of flares to occur, from an extremely impulsive rise to an extremely slow rise, all on the basis of gradient steepness and field magnitudes. The fast-rise flares should occur in regions of steep gradients, and slow-rise flares should occur in regions of weaker gradients. Since in general gradients can be expected to weaken with altitude, *one should expect the most impulsive flares to occur in small compact arches,* and *gradual-rise-and-fall* (GRF) *flares should occur in larger arches, i.e., arches with larger L.* On the other hand, great flares, in the sense of quantity of energy released, should occur in arches with very large currents but not necessarily large gradients, and small flares shoulf occur in arches with smaller currents but not necessarily with weak gradients. Hence on the basis of these relatively trivial arguments we should expect four basic classes of flares originating in arches:

- GRF with small energy release,
- GRF with large energy release,
- impulsive rise with little energy release,
- impulsive rise with large release.

3.2. Mechanisms for Magnetic Energy Conversion

The most crucial question of any flare model is how the stored energy is converted into the kinetic processes associated with a flare. As we have seen, there are basically three means by which current in a diffuse pinch, and therefore an arch, can be converted into kinetic energy: pure MHD modes, resistive MHD modes, and electrostatic instabilities.

Electrostatic instabilities will play a role in our flare model only as mechanisms to alter the transport coefficients. This follows because, if the bulk current were to become electrostatically unstable, the rate of anomalous heating by microturbulence is of the order $\eta_{an} j_T^2 \Delta V$, where η_{an} is the anomalous resistivity resulting from the electrostatic instability. Since ΔV is small observationally, $\leqslant 10^{25}$ cm^3, j_T must be large to explain the energy release, and η is of the order 10^{-13} s. Hence, if $j_T \approx 10^7$ statampères cm^{-2}, $\mathrm{d}\varepsilon/\mathrm{d}t \leqslant 10^{26}$ ergs s^{-1}, which is insufficient to explain a flare unless ΔV or j_1 are increased. In addition, it is easy to show that most MHD

modes will be excited prior to the bulk current becoming electrostatically unstable. Hence one expects the MHD modes to come into play long before the arch current ever becomes electrostatically unstable. Therefore the pure MHD and resistive MHD modes will be of primary concern.

As should be clear, the MHD modes and the resistive modes differ only in that the MHD modes assume an infinite-conductivity model, whereas the resistive modes relax this constraint and in so doing permit instabilities not because they are energetically favorable but because the infinite conductivity constraint excluded them from the outset. Thus we found that once finite conductivity is introduced, a much wider class of instabilities was permitted. We should therefore be careful not to make the mistake of assuming that if a pure MHD mode were to occur, a resistive mode cannot also occur or vice versa. Indeed we should expect both classes of instabilities to occur during the duration of the flare, if conditions are satisfied. Thus, although we emphasize the tearing mode in our discussion of energy conversion, we should still expect MHD kink modes to occur.

3.3. Volume of Energy Release

When we consider the volume within which instability can occur, we have to ask: what is the thickness in minor radius Δr where instability occurs, and over what portion of the arch ΔL should it occur? However, to determine ΔL or Δr requires precise knowledge of the current density and B_T over the whole of the arch. This of course is not known. We can however argue that although Δr and ΔL have certain minimal values initially, they will enlarge as the instability convects out of the region of initial instability. For example as noted in Spicer (1976a) Suydam's condition implies convective mixing outward toward the outside boundary until stable and that this convection should easily occur *because of the small separation of modes due to the scale of the arch.* Further, *because* $\mathbf{k} \cdot \mathbf{B} = 0$ *requires specifying two mode numbers* (k, m), *there are potentially an infinite number of singular layers possible to excite,* particularly if a turbulent spectrum of $\mathbf{k}$ exists which satisfies $\mathbf{k} \cdot \mathbf{B} = 0$. In addition singular layers within a distance δr of one another will have nearly the same mode numbers (k, m) and therefore similar growth rates, if unstable. Hence this region of thickness δr will be subjected to nonlocal quasi-modes, which can greatly increase the volume in which instability occurs. Or, if the amplitudes of the current perturbations which result from the tearing mode are large enough, resonances can overlap, substantially increasing the effective volume and rate of reconnection. We can then conclude that Δr should be much greater than a thickness of a singular layer. Thus we assume $\Delta r \gg \varepsilon a$ and we take $\Delta r \approx r_{\max}/10$, where $r_{\max}$ is the minor radius of the outside boundary of arch, $a \approx (\nabla |B|/|B|)^{-1}$ and εa is the singular layer thickness.

An examination of Equation (3.2) shows that critical current density for kink instability is a function of the location along the arch as well as of r. We should therefore expect there is some length ΔL in which instability will occur. We will let observations of small flares guide us here and assume $\Delta L \approx 1400$ km. Since

r_{max} observationally appears to be of the order 700 km, we have that $\Delta r \approx 70$ km. Hence we will adopt in all the estimates to follow an incremental volume $\Delta V \approx 2\pi r_{max} \Delta r \Delta L \approx 4.3 \times 10^{23}$ cm^3 for a small flare. This necessarily implies $\gamma B_p^2/4\pi$ must be $\gtrsim 10^5$ ergs cm^{-3} s if we are to explain the small-flare energy release, which is typical of the order 10^{30} ergs over 100 s. In addition we will adopt the values $B_p = 500$ gauss, $n = 10^{12}$ cm^{-3}, and $T = 5 \times 10^5$ K as the initial temperature at instability onset. It must be recognized that the adopted values all correspond to the values obtained from flares as observed by the ATM. We will assume for the present that one can explain large flares by an appropriate scaling of these parameters.

In what follows we will assume that conditions existing within the arch are such that the tearing mode can be excited, i.e., $\Delta' > 0$ (Furth *et al.*, 1963). Further, we will use the growth rate corresponding to the fastest growing tearing modes in sheet geometry, i.e., $\alpha = 0.2 = ka$ (Furth *et al.*, 1963) these being the modes we expect to grow first. This implies a growth rate

$$\gamma \approx \frac{1}{\sqrt{\tau_R \tau_H}}. \tag{3.7}$$

We are using sheet geometry only for ease in calculation, since the numerically calculated growth rates for various cylindrical magnetic-field models in (Spicer, 1976a) are difficult to apply in parameterized form. However the growth rates obtained for cylindrical models are generally greater for the same Reynolds number and α. In particular the numerical growth rates appear to be very model dependent; e.g., the force-free BFM with $S \approx 10^6$ and $\alpha = 0.2$ gives $\gamma \approx 10^2$, whereas the sheet pinch gives $\gamma \sim 10$.

Using

$$\tau_R = \frac{4\pi a^2}{\langle \eta \rangle c^2} \tag{3.8}$$

and

$$\tau_H = \frac{a(4\pi p)^{1/2}}{B}, \tag{3.9}$$

where $a \approx (\nabla B_p / B_p)^{-1}$ across the singular layer or layers, we obtain from Equation (3.1)

$$\frac{d\varepsilon}{dt} \approx 1.6 \times 10^{14} \left(\frac{\langle \eta \rangle}{\sqrt{n}} \right)^{1/2} \Delta V \left(\frac{B_p}{a} \right)^{3/2} B_p. \tag{3.10}$$

Consider first the behavior of the energy release when the resistivity is classical. Since $\eta \sim T^{-3/2}$, $d\varepsilon/dt \sim T^{3/4}$, which suggests the energy release by the tearing mode evolves into a state of marginal stability. That is, since $d\varepsilon/dt \sim T^{3/4}$, the rate of energy release drops off and continues to do so until the mechanisms that cool result in a temperature drop, which then drives $d\varepsilon/dt$ back up above the cooling rate, so the instability evolves to a marginal state.

The marginal state will occur at some temperature T_F, at which time

$$\frac{1}{\Delta V}\frac{d\varepsilon}{dt} \approx n m_e v_{T_e}^3 \frac{(T_F)}{\Delta L}, \tag{3.11}$$

where we have used the fact that thermal conduction appears to be the dominant cooling mechanism during flares. Hence near marginal stability the growth rate is given by

$$\gamma(T_F) \approx n m_e v_{T_e}^3 \frac{(T_F) 4\pi}{B_p^2 \Delta L}, \tag{3.12}$$

which is much less than $\gamma(T_{in})$. *We identify this marginal state with the so-called gradual phase of the flare* and *identify the initial growth phase with the impulsive phase or flash phase. Such identifications necessarily imply that the energy release is continuous but decreasing during the gradual phase.*

Inserting the adopted values for T_{in}, n, B_p, and ΔV into Equation (3.10), we obtain

$$\frac{d\varepsilon}{dt} \approx \frac{6.8 \times 10^{33}}{a^{3/2}}. \tag{3.13}$$

A typical small flare releases $\approx 10^{30}$ ergs in a time $\Delta t \approx 100$ s. Thus we require $d\varepsilon/dt \approx 10^{28}$, which implies $a \approx 7.7 \times 10^3$ cm. An $a \approx 7.7 \times 10^3$ cm corresponds to a perturbation with a wavelength $\lambda \approx 10\pi a = 2.4 \times 10^5$ cm if $\alpha = 0.2$. Such a wavelength perturbation will not cause the arch to be globally kink unstable; hence we do not expect these perturbations to cause global kinks in a flaring arch, although longer wavelength kinks can develop and considerably distort the plasma-field configuration macroscopically.

A gradient of the order 7.7×10^3 cm and a $B_p \approx 500$ gauss corresponds to a toroidal current density $j \approx 1 \times 10^8$ statampères cm ^{2} in, or $B_p/a \approx 0.06$ gauss cm^{-1} across, the singular layer: a value $\approx 10^2$ times greater than has been observed in active regions (Title and Andelin, 1971). This value of the field gradient should not however be considered excessive, since the observations typically have a spatial resolution $\gg 700$ km and thus average over the whole of the arch cross section, whereas this value of B_p/a should exist only in a localized region, which, as we will see, can occur because of a rapidly growing current density in the region of instability.

3.4. Anomalous Resistivity and the Energy Release Rate

Using Equation (3.6) and inserting T_{in} and $j \approx 1 \times 10^8$ statampères cm^{-2}, we find that $n \gtrsim 2.26 \times 10^{10}$ cm ^{3} is required for stability against the electrostatic ion sound or ion cyclotron mode. Since we have chosen $n = 10^{12}$, we will satisfy this requirement and the bulk current is electrostatically stable. Similarly the value a obtained earlier also is above the gradient scale for the ion sound instability which yields for the adopted values $a \approx 10^2$ cm. However both of these equivalent

results imply that it may be possible to drive the current electrostatically unstable in the regions around the singular layer. Hence it is important that we consider how anomalous resistivity will affect the rate of energy release.

As discussed by Spicer (1976a) we can expect two types of instabilities that can lead to anomalous resistivity: current driven, either parallel or perpendicular to the magnetic field, and beam driven. We will consider only the parallel current-driven and beam-driven instabilities, while noting that the cross-field-driven instabilities have thresholds similar to the parallel-field-driven instabilities and as such will yield similar results. However a more correct treatment of current-driven anomalous resistivity would examine $j_\perp$-driven instabilities, since the current is flowing perpendicular to B near the singular layer. But because the magnetic field changes sign at $\mathbf{k} \cdot \mathbf{B} = 0$, it is small there, and we will neglect it to first order.

Let us assume that the parallel-field current-driven ion sound instability is excited and that $T_e/T_i \approx 10$. The a required for instability is

$$a \lesssim \frac{c}{\omega_{pi}} \left(\frac{1}{\beta_p}\right)^{1/2} \frac{1}{1 + \left(\frac{T_e}{T_i}\frac{m_i}{m_e}\right)^{1/2} \exp\left(-\frac{T_3}{2T_i}\right)}, \tag{3.14}$$

which for the adopted values yields $a \approx 1.4 \times 10^2$. Such a gradient corresponds to $j_T \approx 8.53 \times 10^9$ statampères cm^{-2} or $B/a \approx 3.57$ gauss cm^{-1} in or across the singular layer. Such a field gradient is not likely to be found along the whole length of arch but rather in a well localized region and will act as a localized current interruption or discharge, generating localized voltage drops along the singular layers.

These regions will expand somewhat, since the unstable waves of the excited instability will propagate out of the region of instability, at their group velocity, into a region where they are stable. Within these small regions the resistivity will be anomalous, and the instability exciting the anomalous resistivity, here assumed to be the ion sound instability, will saturate in a few ion plasma times to a state of marginal stability. Hence within these regions one should expect extreme localized heating much greater than in the regions where the resistivity is classical. However it is unlikely that the bulk current across the total cross section of the arch will become electrostatically unstable, because of the steep gradients required.

Since the effective collision frequency, due to the current-driven turbulence, goes typically as $\nu_{\text{eff}} \sim A\omega_{pe}$, the growth rate of the tearing mode in the presence of this bulk current-driven anomalous resistivity will be dominated by the density, so that $\gamma \sim n^{-1/2}$ rather than $\gamma \sim T^{-3/4}$. Equation (3.1) becomes

$$\frac{1}{\Delta V}\frac{\mathrm{d}\varepsilon}{\mathrm{d}t} \approx 10^{10} \left[\frac{A}{n}\right]^{1/2} \left(\frac{B_p}{a}\right)^{3/2} B_p, \tag{3.15}$$

where A for the ion sound instability is of the order 1/100. Using the adopted values for n and B_p and $a \approx 10^2$ cm, we find

$$\frac{1}{\Delta V}\frac{d\varepsilon}{dt} \approx 4.26 \times 10^7 \text{ ergs cm}^{-3}\text{ s}^{-1}, \tag{3.16}$$

which is approximately 10^2 greater than if the resistivity were classical.

If the flare were due only to these small regions within the arch, then the volume of instability would be $\approx 10^{20}$ cm^3, or if a given flare resulted from a combination of tearing modes dominated by classical and anomalous resistivity, that particular flare would show evidence of extremely intense emission within regions 5×10^7 cm^2 in cross section and length $\geq 10^5$ cm.

However the heating at the onset of anomalous resistivity is dominated not by the tearing mode but by the current-driven microinstability, since the growth rates for these microinstabilities are so much greater than the growth rates for any macroinstabilities. Thus the temperature within an electrostatically unstable singular layer will grow impulsively at a rate

$$\frac{\partial T_e}{\partial t} \approx \gamma_{\text{micro}} T_e. \tag{3.17}$$

After saturation of the microinstability, which occurs in a few ω_{pi}, the heating rate by the microinstability is given by

$$nk\frac{\partial T_e}{\partial t} \approx \eta_{AN} j_T^2, \tag{3.18}$$

which is of the order 7×10^5 ergs cm^{-3} s^{-1} within the electrostatically unstable singular layer. This heating however is dominated by the tearing-mode energy release, which in turn is dominated within these singular layers by anomalous resistivity, as given by Equation (3.15).

Let us summarize what we have found as far as energy release is concerned. We have considered two cases: an electrostatically stable bulk current which leads to a flare by the tearing mode dominated by classical resistivity, and an electrostatically unstable current occurring only in some singular layers while the remaining singular layers remain electrostatically stable. This second case results in what should be construed as nonthermal heating within the electrostatically unstable singular layers. Further, the total volume occupied by all the singular layers dominated by anomalous resistivity is $\approx 10^{20}$ cm^3, which is $\approx 10^{-5}$ less than the resolution-limited volume of $\leq 10^{25}$ cm^3 reported by the Skylab observers whereas the volume required to explain the flare with a classical resistivity dominated energy release was 10^{23} cm^3, which is $\approx 10^2$ less than the observed volume. However present observations do not require that we invoke bulk current-driven anomalous resistivity to explain the flare energy, nor do present observations support the assumptions of such gradients. Hence we will no comment on this further.

Let us now consider a source of anomalous resistivity that is generated by a nonthermal beam trapped in a current-carrying arch, as developed by Papadopoulous and Coffey (1974a, b). If this beam is inhibited from relaxing quasilinearly by nonlinear processes, the beam will represent a nonthermal driving mechanism, capable of producing ion density fluctuations. The particular nonlinear process considered by Papadopoulous and Coffey is the parametric oscillating two-stream instability (OTS). The requirement that OTS stabilizes the beam before the quasilinear relaxation of the beam occurs is given by

$$\frac{\Delta v_b}{v_b} \geqslant \left[10^2 \left(\frac{n_b}{n}\right)^{2/3} \left(\frac{v_{T_e}}{v_b}\right)^{2/3} \left(\frac{mi}{m_e}\right)^{1/3} (k_m \lambda_d)^{-2/3} \right]^{3/7}, \tag{3.19}$$

where v_b is the beam velocity, Δv_b is the beam thermal spread, n_b is the beam density, and $k_m \lambda_d \approx 0.15$, k_m being the wave number with the maximum growth rate.

The assumption that a beam exists in an arch (the origins of such a beam will be discussed in Section 5) with $v_b \approx 10^{10}\ \mathrm{cm\ s^{-1}}$ and $T_e \approx 10^6\ \mathrm{K}$ yields

$$\frac{\Delta v_b}{v_b} \geqslant 10 \left(\frac{n_b}{n}\right)^{2/7}. \tag{3.20}$$

If $\Delta v_b / v_b \approx \frac{1}{3}$ and $n \approx 10^{12}\ \mathrm{cm^{-3}}$, Equation (3.20) implies $n_b \leqslant 7 \times 10^6\ \mathrm{cm}^{-3}$ if the beam is to be stable against quasi-linear relaxation. If such a beam exists within the arch, it will lead to purely growing ion-density fluctuations with an effective collision frequency

$$\nu_{\mathrm{eff}} \approx 2 \left(\frac{\pi}{2}\right)^{1/2} \omega_{pe} (k_m \lambda_d) \left(\frac{n_b}{n}\right) \left(\frac{v_b}{v_{T_e}}\right)^2 \frac{\Delta v_b}{v_b} \tag{3.21}$$

(Papadopoulas and Coffey, 1974b). Using the values previously obtained, we have that

$$\nu_{\mathrm{eff}} \approx 86.7 \omega_{pe} \left(\frac{n_b}{n}\right). \tag{3.22}$$

As noted by Papadopoulos and Coffey, Equations (3.21) and (3.22) show that the anomalous resistivity is proportional to the beam energy, and for fixed beam energy the resistivity scales as $n^{1/2}$. Thus the anomalous resistivity will be a decreasing function of altitude in the arch.

Since the Coulomb collision frequency $\nu_{ei} \approx 80 n T_e^{-3/2}$, we find for $T_e \approx 5 \times 10^5\ \mathrm{K}$, $n \approx 10^{12}\ \mathrm{cm^{-3}}$, and $n_b/n \approx 10^{-6}$ that

$$\frac{\nu_{\mathrm{eff}}}{\nu_{ei}} \approx 3 \times 10^2. \tag{3.23}$$

Hence we expect the bulk resistivity η to increase by $\approx 3 \times 10^2$ over its classical value. Using Equation (3.10), we find that the energy release will increase by a factor of 17 over those values obtained when the resistivity was assumed classical.

Since the time scales for beam stabilization by OTS are so short, a quasi-steady state should be established so together the beam plasma and parametric instabilities will evolve to a marginally stable state. Thus the bulk anomalous resistivity generated by the beam will exist with a ν_{eff} given by Equation (3.22) over the duration of the beam. However the effectiveness of this mechanism is clearly related to lifetime of the beam, or the period of time in which beam replenishment occurs, as well as the cross sectional area in which the beam exists. Since these questions are clearly related to the origins of the beam, we will postpone its discussion until we take up the question of flare precusors.

We are now in a position to estimate the size of the arch. Taking the adopted value of B_p and taking the total energy release during a small flare to be $\approx 10^{30}$ ergs, we find the total storage volume required is of the order 5×10^{25} cm^3, which is relatively small.

If the volume of the observed arches is greater than this, with $B_p \sim 500$ gauss, the arch will have sufficient volume to store the energy necessary to explain the energy release. If the volume is less than this, a current reservoir must exist beneath the photosphere which maintains the current throughout the flare duration.

If we take $2\pi r/L \approx \pi/5$, with $B_p \approx 500$ gauss we require $B_T \gg 795$ gauss, if the arch is to be MHD stable prior to flaring. A ratio of $r/L \approx \frac{1}{10}$, using $L \approx \pi R$, we find $R \approx 3 \times 10^8$ cm. Hence, the arch will have an altitude of the order 3000 km for the small flare considered.

We will conclude this section by discussing briefly the validity of Equation (3.1). First, it should be obvious that the use of

$$\frac{d\varepsilon}{dt} \approx \frac{\gamma B_p^2 \Delta V}{4\pi}$$

sweeps many problems under the rug. It ignores the fact that one should expect things like nonlinear mode coupling between primary resonances, secondary resonances, etc. which occur by generating higher harmonics and subharmonics of the original modes. Everything else being equal, these higher harmonics necessarily have greater growth rates. In addition Equation (3.1) ignores the fact that different singular layers are tearing at different places at different times within the flare volume. Or, to put it otherwise, Equation (3.1) averages over a multitude of sins which the complexities of the physics and mathematics forces on the physicist.

4. The Formation of Impulsive Electromagnetic Bursts and Shocks

As is clear from Section 3, the mechanisms we have proposed for the thermalization of the magnetic field in an arch are more than adequate to explain the total energy release of a flare. *If these thermalization mechanisms were to lead to a thermal plasma only, our model could explain only the thermal flare,* i.e., *those flares that do not lead to impulsive electromagnetic bursts* (IEBs) *and to shocks.*

Hence the purpose of this section is to examine the means by which MHD and resistive MHD instabilities can lead to IEBs and to shocks.

As a way of introduction to what we feel is a more realistic explanation of IEBs, we briefly illustrate a well-known laboratory phenomenon that has many features similar to those that occur during a nonthermal flare.

Figure 4 illustrates the X-ray trace, obtained from the ST Tokamak (von Goeler *et al.*, 1974), generated by an instability referred to as the disruptive instability. This figure illustrates two things: an extended X-ray burst and, superimposed on it, impulsive X-ray bursts. The similarity between this laboratory phenomenon and the impulsive flare should be obvious and appears to be quite significant. First, the explanation of this impulsive behavior, as we will discuss in more detail, is believed to result from a combination of MHD and resistive MHD modes, and, second, the bremsstrahlung bursts are not due to just accelerated particles but rather from both intense thermalization of the magnetic fields and electron acceleration in the induced electric fields generated during instability. Hence soft and hard components of these IEBs exist, *both emanating from the same volume.*

4.1. Thermal or Nonthermal Flares

To make clear what we mean by thermal and nonthermal flares, we examine under what circumstances the tearing mode is a thermal or nonthermal process. The defination we will adopt is: a thermal plasma is a plasma in which relaxation between like species has occurred or in which the approach to relaxation has reached some semblance of a steady state. Hence a necessary condition for the heating to be nonthermal is: the heating per particle per second must exceed the

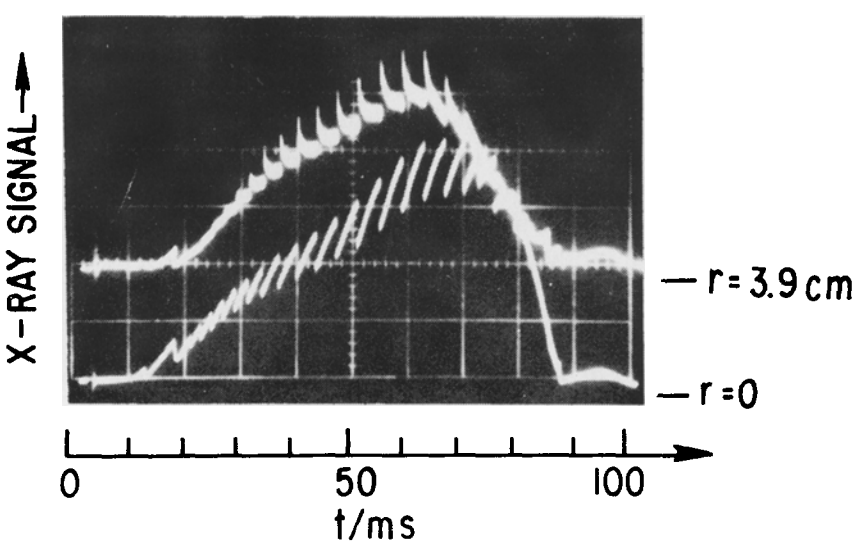

Fig. 4. X-ray trace due to disruptive instability.

rate at which relaxation occurs between like species. In our case the species of interest is the electron.

The above definition implies that the tearing mode will act as a nonthermal heating mechanism for electrons if

$$\frac{\gamma B_p^2}{4\pi n_s} > \nu_{ee} k T_e, \tag{4.1}$$

where n_s is the number density of these electrons in 'resonance' with the tearing mode and ν_{ee}^{-1} is the relaxation time between electrons, defined (Spitzer, 1967) as

$$\nu_{ee}^{-1} \approx 0.266 \frac{T_e^{3/2}(\mathrm{K})}{n_e \ln b} \mathrm{s}. \tag{4.2}$$

Equation (4.1) states that those electrons in resonance with the tearing mode will be heated at a faster rate than electron–electron collisions can relax the electron distribution. Generally only the fast-growing short-wavelength tearing modes will satisfy this condition.

Equation (4.1) has a number of consequences which can better define the origins of the thermal and nonthermal flares. Clearly the larger the ambient density, the harder (4.1) is to satisfy, and the larger the B_p and γ, the easier (4.1) is to satisfy. Since we expect B_p and γ to increase as we descend in altitude and n to decrease as we ascend in altitude, *there should exist an annulus, with a thickness Δh in altitude and mean altitude h, within which nonthermal flares generally occur.*

Using the adopted values from Section 3, we find the energy transmitted to an electron per second, by the tearing mode, is of the order 86 keV s^{-1}, if $n_s = n$. This rate of nonthermal hearing is more than sufficient to explain the observations.

The tearing mode will also accelerate a selected few electrons by the induced low frequency electric fields, generated during reconnection. The magnitude of these electric fields, and the subsequent energy gains $\Delta\varepsilon$ can be crudely obtained from Faraday's equation. We obtain $\Delta\varepsilon \approx e\gamma B_p a^2 2\pi/c\alpha$, and using the values adopted for B_p, γ, a, and α, we find a maximum energy gain of the order 2 MeV.

It should be emphasized that because the induced electric fields generated by the tearing mode have a low frequency they appear as DC electric fields to the electrons and ions and can therefore accelerate the particles to high energies, even though a driven two stream instability will result (Spicer, 1976b).

4.2. Mechanisms that can form IEBs and shocks

As noted, nonthermal flares are invariably associated with shocks. This is highly suggestive, because the formation of a shock requires a sudden increase in pressure, and to form such a pressure pulse requires either that the flare heating mechanism rapidly thermalize part of the stored energy or that rapid motion of the bulk plasma takes place. We consider both these possibilities.

If we require the impulsively heated and/or accelerated electrons and shocks to emanate from the same thermalization volume within the arch, we must also

require the conversion of potential energy to kinetic energy be extremely rapid during their formation. This suggests the difference between the thermal and nonthermal flare lies in the rate of energy conversion per unit volume. Since the greater the conversion rate for this model, the greater the rate of current dissipation, it follows that during such rapid dissipation the magnitudes of the expected current perturbations by the tearing mode are also greater. Hence the likelihood of nonlinear resonant overlap is greatest in this situation. A consequence of overlap is to increase the degree of reconnection per unit volume substantially, increasing the rate at which magnetic energy is thermalized per unit volume.

Nonlinear resonant overlap, we have noted will result in abrupt and dramatic increases in the rate of reconnection. During overlap we can therefore expect impulsive heating and acceleration at rates which are much greater than linear analysis would predict. overlap should also increase in likelihood of (4.1) being satisfied.

Finn (1975) has calculated the magnitude of the required current perturbations for overlap of the $m=2$ islands and $m=3$ islands for a peaked current model (Furth *et al.*, 1973). He found that the perturbations necessary were typically $\approx 1.5\%$. For a less peaked current profile (less shear) Finn found somewhat larger current perturbations necessary (4%). These studies illustrate that relatively weak perturbations can lead to resonant overlap and may play a very important role in flares.

An alternate as well as complementary means by which this model can generate IEBs and shocks is global kink modes. That is, the whole arch or a substantial portion of it may undergo kinking, leading to a strong disruption of the bound plasma. Since a kinking arch will produce effects similar to the disruptive instability previously mentioned, this would be an appropriate place to include it in our discussion.

The disruptive instability (DI) develops when the toroidal current in a tokamak causes the safety factor q at the plasma boundary to be small, i.e., $q \approx 3$ or 4. The DI manifests itself either as singular or quasi-periodic abrupt changes in the plasma parameters. These changes are a result of a slow $m=1$, $n=1$ internal kink mode which has a growth rate $\gamma \approx v_A/R$. During the growth X-rays are formed which are suddenly reduced in magnitude because of a rapid cooling in the central region of the Tokamak. This cooling disruption appears as a symmetric $m=0$, $n=0$ mode (in an arch the $n=0$ mode is forbidden, although the $m=0$, $n=1$ mode can occur). After the cooling disruption a slow process of relaxation sets in with $q<1$ at the magnetic axis, i.e., $r=0$, and the whole sequence may repeat itself.

Kadomtsev (1976) has recently proposed a new explanation for this phenomenon. Qualitatively Kadomtsev argues that as the internal kink grows, it will compress neighboring magnetic surfaces to one side, which then undergo resistive kink modes and thus reconnection. As the kink attempts to stabilize itself, it will

nonlinearly swing back and forth between stability and instability. During this period the reconnection process will repeat itself quasi-periodically, so the magnetic field dissipated will appear as impulsive joule heating and subsequently as X-rays. If the distortion of the magnetic surfaces by the kink modes is great enough, the kink can cause resonant overlap with an accompaning increase in field dissipation and subsequent heating. This should be especially true in an arch, because of the close spacing of the modes.

If we apply these ideas to an arch, we find similar effects. Since a kink oscillates with a frequency of the order $f \approx 2\pi/kv_A$, we find for the $m = 1$, $n = 1$ mode $f = L/v_A$. This corresponds to a frequency range of about 1 to 30 s, the exact magnitude being determined by the local conditions within the arch.

If the kink were an external kink rather than an internal kink, the kink could thrash about, causing shock waves in the ambient atmosphere. If these shocks have a large enough Mach number, the shocks can excite various two-stream instabilities (Tidman and Krall, 1971), thereby causing a rapid 'thermalization' of the shock's ordered energy. Hence, in this case, one should expect bursts of bremsstrahlung with a period similar to those obtained earlier.

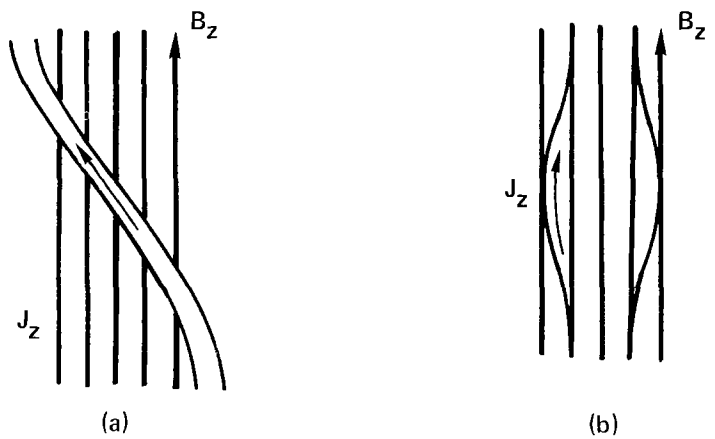

Fig. 5. Resistive instabilities for a diffuse pinch: (a) stabilized pinch with kink in $J_z(m = 1)$; (b) stabilized pinch with sausage in $J_z(m = 0)$.

If the kink were instead a resistive kink which formed on the plasma boundary of the arch, as depicted for a diffuse pinch in Figure 5 and for an arch in Figure 6, it could explain why impulsive X-ray bursts and type III bursts sometimes appear in groups, five type III bursts and five X-ray bursts with similar structure. This follows because an MHD kink results in a strong distortion of the plasma column and in so doing results in an appreciable induced electric field, which can accelerate particles (Glasstone and Lovberg, 1960).

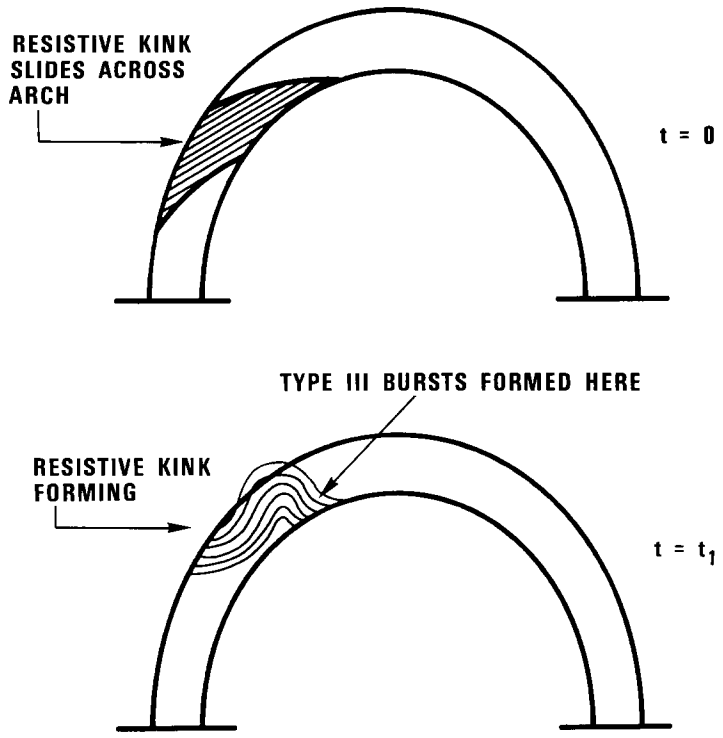

Fig. 6. Type III bursts and resistive sheet kink.

A similar situation can occur when resistivity is taken into account. Here a kinking current sheet will be formed at the boundary of the plasma column and will slide across the column as it kinks (Figure 5). Hence the electrons can escape from the sheet as the sheet undergoes resistive kinking. However, for this mechanism to explain the repetitive behavoir typical of many type III chains, the wavelength of the kinking portion of the arch must be much less than the arch length, so as the kink thrashes back and forth, it will accelerate electrons in bursts with the proper frequency $f \approx 2\pi/k v_A$. If such behavior should be observed and is correlated with type III bursts, it will be strong evidence in support of this resistive-kink flare model.

The formation of IEBs by the above mechanisms has a number of advantages over the standard explanation that IEBs form by electron deposition into the denser atmosphere beneath the acceleration site. These advantages are:

– There is no need to find an exotic acceleration mechanism that accelerates only electrons with a 90 to 100% efficiency;

– we need not accelerate $\approx 10^{39}$ electrons to form the IEBs, as required by the deposition hypothesis, since the same electrons can be repeatedly heated and/or accelerated within the same volume (the accelerated electrons being stopped quickly by the high arch densities);

– we need not develop separate mechanisms to form IEBs and shocks, since they appear together as a natural consequence;

– we can show that similar behavior manifests itself in laboratory experiments, serving as a guide to our understanding.

In summary we have argued that IEBs and shocks can result from impulsive heating and/or acceleration. This explanation we believe is more natural than previous explanations.

4.3. Other modulation mechanisms

One odd thing about nonthermal flares is that occasionally chains of type III bursts are formed, the bursts sometimes being separated by intervals of $\leqslant 1$ s. Since the type III burst results from an electron stream, these chains may be simply a result of pinching instabilities to which electron streams are inherently subject. However, although this explanation may be correct, there are two other means by which one could explain these chains within the context of this model.

Consider first the MHD $m = 0$ mode. As discussed by Glasstone and Lovberg (1960), this mode in the presence of a stabilizing axial field B_z is known to oscillate with a frequency

$$\omega^2 \approx \frac{B^2}{4\pi r_l \rho_s}, \tag{4.3}$$

where r_l is the equilibrium pinch radius, B is the magnitude of $\mathbf{B}$, and ρ_s is the surface density of the current sheath which is assumed to exist at the equilibrium radius. These oscillations, unlike the $m = 0$ oscillation in the unstabilized pinch ($B_z = 0$), are usually small but discernible. However they generally do not generate the radial shocks characteristic of the unstabilized pinch.

Since the period of oscillation that is characteristic of the observed quasi-periodic bursts is typically about 1 to 10 s, and we adopted a value for $B \approx$ 500 gauss, we find that $r_l \rho_s \approx 10^{28}$. This implies both the equilibrium radius of the arch and its length must be large. Using a value of $r_l \approx 10^8$ cm, and demanding the period be of the order 10 s, we find the $m = 0$ mode will induce an electric field

$$E_T \approx \frac{r_l B_p}{c}. \tag{4.4}$$

which gives $E_T \approx 10^{-2}$ statvolts cm^{-1}. The energy accumulated by these particles per oscillation is $\varepsilon \approx 5 \Delta L$ (eV), where ΔL is the length in centimeters of the region where B_p is changing within the sausage. Thus, if an arch were sausage-mode unstable, it can generated modulated-heated and accelerated electrons of reasonably high energy, with a period given by (4.3).

An alternate cause of quasi-periodic bursts may be the fusing of one or more island chains formed at the resonant surfaces $q = m$. The associated rapid change of magnetic flux as the islands are fused will produce voltage spikes due to flux changes, i.e., $V = \mathrm{d}\Phi/\mathrm{d}t$, where $\Phi = 1/c \int \mathbf{B} \cdot \mathrm{d}\mathbf{S}$.

The evolution of an island chain is as follows: Short wavelengths island chains are formed first during the evolution of the tearing mode, because the shorter wavelength islands have a much greater growth rate than the longer wavelength islands. These short-wavelength islands then represent parallel filaments, which then fuse to form lower energy and slower growing islands (Figure 7). This process repeats itself until the lowest energy longest wavelength is reached. Investigations by Finn and Kaw (1976) have shown that fusing of islands will occur at the fast MHD rate, when the forces of fusion overwhelm the stabilizing forces, due to the compression of the magnetic field between islands. We can treat this phenomena in a semiquantitative form by developing a circuit analog to the problem. To do this we can introduce lump circuit parameters to describe the physical mechanisms at work in a plasma. Following Tidman and Stamper (1973), we convert the electron momentum equation to the form

$$V = IR + \frac{\mathrm{d}(IL)}{\mathrm{d}t} + \frac{I\,\mathrm{d}t}{C}, \tag{4.5}$$

where I is the total current, R is the total resistance, L is the inductance, and C is the plasma capacitance. Recognizing that a magnetic island represents a circuit filament, we can treat each island as a conducting wire with a self-inductance and a mutual inductance between differing islands. First we assume each island is part of one island chain on a resonant surface $q = m$, so that each island is in parallel. The inductance of multiple conductors may be found from circuit theory, using

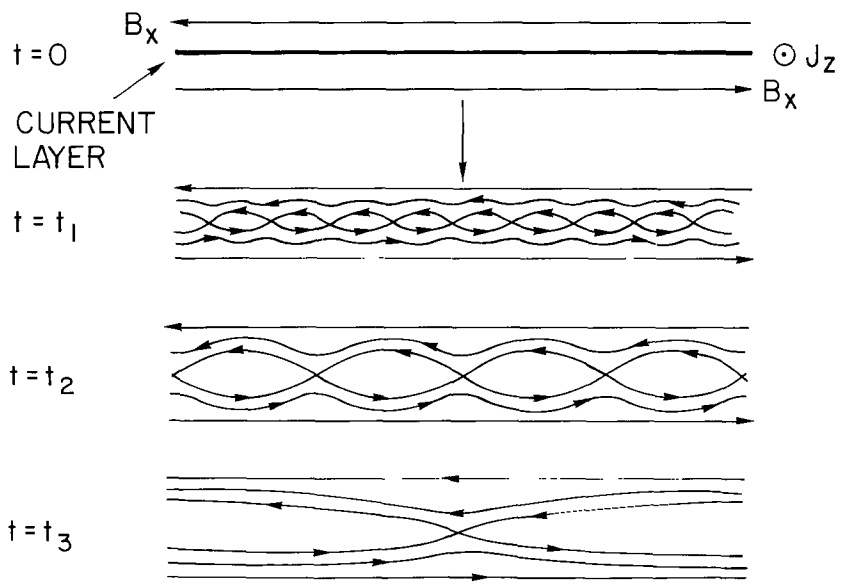

Fig. 7. Evolution of the tearing mode.

formulas for the self-inductance of a straight conductor and for the mutual inductance of parallel conductors. In our simple case, that of m equal wires corresponding to m islands spaced uniformly on a circle whose radius is determined by $q = m$ and connected in parallel, the inductance is given (Grover, 1946) by

$$L = 0.002\,\Delta L \left[\ln\left(\frac{2\,\Delta L}{r}\right) - 1 \right]_{\text{microhenries}}, \tag{4.6}$$

where

$$R = (r m r_s^{m-1})^{1/m}, \tag{4.7}$$

in which $r = \ln \rho - \frac{1}{4}$, ρ being the mean island radius, and in which r_s corresponds to the radius of the resonant surface. When the islands fuse, we expect a voltage drop

$$V(t) = \frac{I\,\mathrm{d}L(t)}{\mathrm{d}t}, \tag{4.8}$$

assuming I is constant.

Typically in conventional electric circuits inductances are constant, so that the $\mathrm{d}L/\mathrm{d}t$ term is zero. However in plasma configurations this is not the general situation, and one finds rather novel electrical behavior. Indeed, as noted by Glasstone and Lovberg (1960), the $I\,\mathrm{d}L/\mathrm{d}t$ term is commonly much larger than the voltage driving the circuit. It is from this term we expect the chains of voltage spikes to have their origins. To see this, assume that Δm islands fuse in a time Δt. Differentiating Equation (4.6) with respect to time gives

$$\frac{\mathrm{d}L}{\mathrm{d}t} \approx 0.002\,\frac{\Delta L}{R}\,\frac{\mathrm{d}R}{\mathrm{d}m}\,\frac{\Delta m}{\Delta t}, \tag{4.9}$$

which leads to Δm voltage spikes every Δt seconds. Assuming $\Delta t \approx \gamma^{-1}$, where γ is the rate of island fusion, we expect $\Delta m \gamma$ voltage spikes per second. These voltage spikes will lead to Δm bursts of heated and accelerated electrons per second, which will appear as a chain of bursts when an island chain fuses to from the lowest energy island. Since other island chains can fuse, more than one chain of bursts can occur.

Estimating the magnitude of Equation (4.8) is difficult, since the total current is distributed throughout the cross section of the arch; and each island when it forms will have a portion of the total current, which differs from that of its neighbor on a different resonant surface. However it is not difficult to convince oneself that the maximum energy gained by a charged particle during these voltage changes is of the order 2 MeV found earlier, and the time between bursts is like an MHD growth time, which is of the order 1 to 10 s, depending on the wavelength of the mode.

5. Flare Model Precursors

The role of precursors is of particular importance in this model, because the precursor mechanisms must set up conditions for onset of the MHD and resistive MHD instabilities used to explain the energy release of the flare. Since these instabilities are driven by $j_{\parallel}$, we shall be interested in mechanisms that can modify the radial-current-density profile. As discussed in Spicer (1976a), a perturbation in $j_{\parallel}$ is directly related to perturbations in either electron density or electron temperature and to the driving electric field.

An examination of the possible mechanisms for altering the current density requires a knowledge of the sources of the current. One can conveniently but somewhat artifically split the possible sources of current into those that occur in or above the photosphere and those that occur below in the convection zone or deeper. Examples of mechanisms that can cause currents by motion of the photospheric fluid are: shearing of one foot of an arch with respect to the other, the differential rotation of one foot of the arch with respect to the other, and the rotation of the individual feet of the arch (Figure 8).

Mechanisms that may cause currents to flow in the convection zone are poorly understood and can only be assumed to exist. This assumption however is reasonable, since the fluid in this zone is a partially ionized plasma with anisotropic transport coefficients much like the ionosphere. Hence, due to collisons with neutral particles, electrons and ions can move across field lines in the convection zone, with different velocities and directions, thereby generating currents. Under these circumstances the current will have large components perpendicular to **B**, and the force-free behavior usually assumed in the solar atmosphere has absolutely no validity in the convection zone or in most of the photosphere.

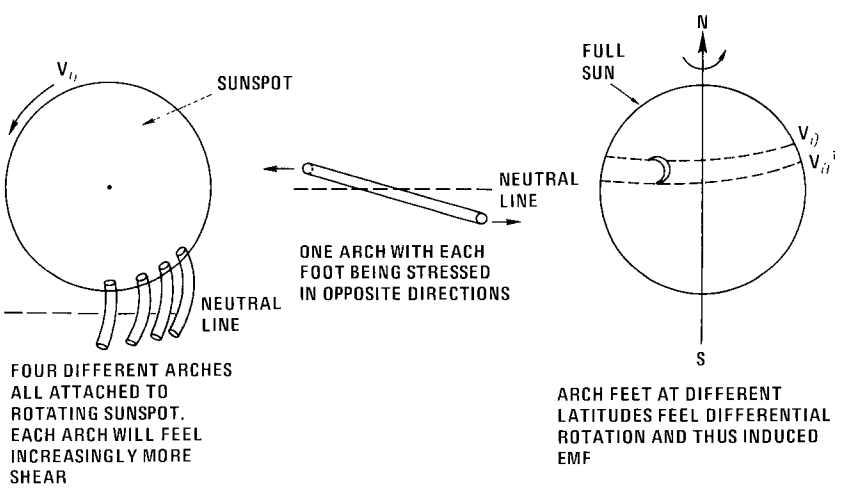

Fig. 8. Examples of photospheric-fluid motion that can cause currents.

Further, if *one believes the typical models of solar magnetism, a safe assumption is that the magnetic topology is multiply connected in the subphotospheric zones and represents an enormous reservoir of stored energy in the form of currents, so that the source of flare energy which is released in situ above the photosphere need not be totally stored there.* Consequently we will assume that a current does exist in the convection zone and that this current can be carried up with the magnetic tubes of force into the solar atmosphere.

5.1. Parametric excitation of MHD kink or resistive kink modes

It is interesting to consider how one might parametrically excite the MHD kink and resistive kink modes. To excite these modes, there must be a coupling to an imposed oscillation, i.e., a pump wave. This parametric coupling is provided by nonlinear effects, and to make these modes grow, one must feed energy to them at a rate which exceeds the rate at which energy is dissipated for the mode in question. Thus, to excite these modes parametrically, the amplitude of the pump has to exceed a certain threshold.

Recent work in dynamic stabilization of kink modes in CTR (controlled-thermonuclear-research) devices has shown that dynamic stabilization, as well as destabilization, can occur by parametric resonances (e.g., Keller *et al.*, 1976). For example the excitation and suppression of kink modes by coupling to ion sound waves has been shown to be possible (Guzdar *et al.*, 1975). This is accomplished by generating a torsional Alfvén wave, whose azimuthal field B_Φ has an associated velocity V_Φ, leading to a relative shear between concentric layers. The Alfvén wave leads to a coupling between the kink modes and ion-sound modes. If the ion sound modes are growing, they can pass their energy to kink modes, thereby driving them unstable. Thus it appears possible that waves from the photosphere can lead to eventual instability in the arch. Undoubtedly other means exist to parametrically excite kink modes.

Parametric excitation of kink modes is of particular interest in the arch, because the spacing between normal modes of the system will generally be very small because of the large size of the arch. Thus it will be much easier to find modes which are close enough together so as to satisfy the resonance conditions and thus become parametrically excited.

A twisting of the arch can produce torsional Alfvén waves. However the existence of growing ion sound waves in an arch is in doubt unless $T_e \gg T_i$, although growing acoustic waves are a possibility, since they satisfy a dispersion relation similar to the ion sound waves. Hence it may be possible for acoustic waves to couple with the torsional Alfvén wave and excite the kink modes.

5.2. Alteration of the current profile in the arch

Let us examine mechanisms and perturbations that will alter the current-density profile of an existing arch, *assuming it is still evolving.* The simplest types of perturbations that immediately come to mind are those perturbations that satisfy

$\mathbf{k} \cdot \mathbf{B} = 0$, i.e., perturbations which are slowly varying in the toroidal directions. One such mechanism is a magnetosonic wave generated by perturbations internally or external to the arch. For example, if a Moreton wave generated by another flare were to strike the arch, it could very easily give rise to magnetosonic waves propagating perpendicular to **B** which would compress the magnetic surfaces, exciting the tearing mode, or which could cause the arch to kink.

An alternate mechanism, using magnetosonic waves, is the conversion of Alfvén waves into magnetosonic waves, as the Alfvén waves propagate along the twisted field lines of the arch. This requires the wavelength of the original Alfvén wave to be less than the local or global curvature. Such a mechanism has been proposed by Wentzel (1974) as a source of heating in arches. The wavelength of the Alfvén waves required are such that $\lambda < R$ and/or $\lambda < rB_T^2/B_p^2$ so as to satisfy the WKB approximation used in Wentzel's analysis. We will comment more on this later. However we are interested in all perturbations that have long wavelengths parallel to **B** along the arch so that thermal conduction will not play an important role, thereby permitting resistive instabilities such as the superheating instability to occur, which we consider next.

The superheating instability is a resistive instability that grows only when $k_\parallel \to 0$, i.e., $\mathbf{k} \cdot \mathbf{B} = 0$. Thus, when this instability does occur, the current density within the singular layer will grow. Assuming the resistivity is classical, the condition for growth is

$$\frac{3j_0^2}{2\sigma_0 T} > \frac{dQ}{dT_0}, \tag{5.1}$$

where $Q \approx P_{\text{rad}}$ and we have neglected the $k_\perp^2 \chi_\perp^2$ term due to thermal conduction perpendicular to the field lines. Rewriting Equation (5.1) as

$$\frac{j_0^2}{\sigma_0} > \frac{2P_{\text{rad}}}{3}, \tag{5.2}$$

where $P_{\text{rad}} = n_0^2 f(T)$, we can obtain $f(T)$ from Figure 9. Since $j_0 = en_0 v_d$ we can rewrite Equation (5.2) as

$$v_d^2 > \frac{f(T)}{e^2 \eta} = 2T_e^{2/3}(\text{eV}) f(T) \frac{3.77 \times 10^{32}}{3Z \ln \Omega}. \tag{5.3}$$

Note that the condition for growth expressed by Equation (5.3) is independent of density.

An examination of the radiation power function for the solar corona (Figure 9), shows that thermal instability is most likely to occur when $T \geqslant 10^5$ K, which corresponds to $f(T) \approx 3 \times 10^{-22}$ erg cm^{-3} s^{-1}. Inserting these values for T and $f(T)$ into Equation (5.3) shows that $v_d > 4.98 \times 10^5$ cm s^{-1}, if the superheating instability is to occur. Requiring a number density of 10^{12} cm^{-3}, yields a current density around $\mathbf{k} \cdot \mathbf{B} = 0$ of $j_T \approx 2.4 \times 10^8$ statampères cm^{-2}, which is very nearly the value found to be necessary to explain the energy release of the flare by the tearing

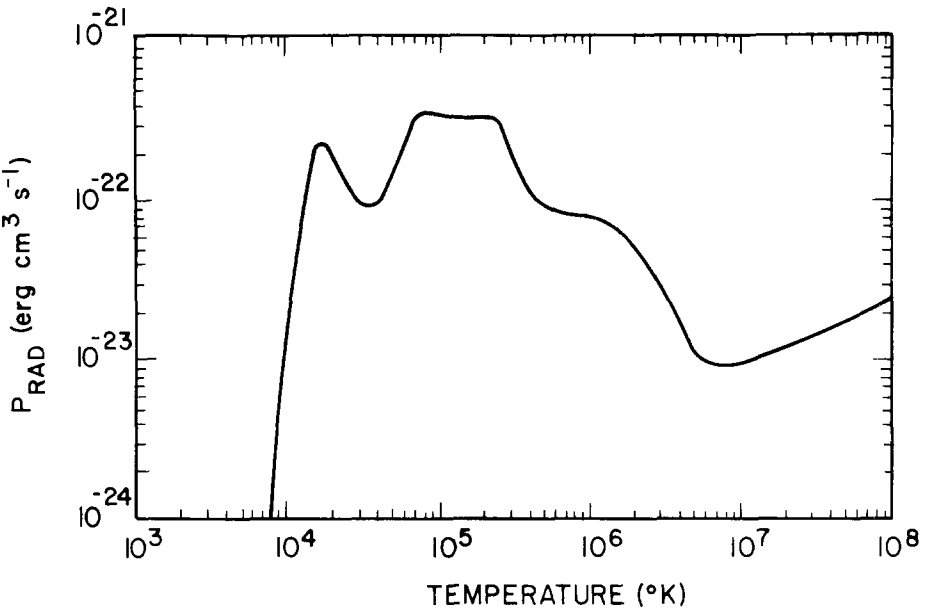

Fig. 9. The radiation power function of the solar corona (McWhirter *et al.*, 1974). The power radiated per unit volume is $n_e n(H') P_{rad}$ erg cm^{-3} s^{-1}.

mode. This corresponds to a growth rate for the superheating instability of $\gamma \approx 2.07 \times 10^{-1}$ s^{-1} or one e-folding time of 4.8 s. If the arch had a lower number density, for example at its outer boundary, it would have a correspondingly lower critical current density and growth rate. For example, if $n \approx 10^9$ cm^{-3}, we must have $j_T \approx 2.39 \times 10^5$ statampères cm^{-2}, which is close to the value reported by Title and Andelin (1970). The superheating growth rate would be $\gamma \approx 2 \times 10^{-4}$ s^{-1}, or one e-fold time of 1.34 hr. Since superheating will cause the temperature to increase, it will produce a temperature gradient across $\mathbf{k} \cdot \mathbf{B} = 0$ such that the resistivity gradient will have a minimum there, which is one of the criteria for the rippling-mode or current-convective instabilities. Assuming the rippling mode is excited, we find that for the adopted values of B, a, n, and T the limits on the growth rate for the rippling mode lie within the range $(9 \leq \gamma \leq 7.43 \times 10^2)$ s^{-1}. Hence, this mode can greatly enhance the growth of the current within the singular layer before it saturates.

To excite these modes again requires perturbations that satisfy the condition $\mathbf{k} \cdot \mathbf{B} = 0$. As already noted, magnetosonic waves can accomplish this by bringing the temperature around $\mathbf{k} \cdot \mathbf{B} = 0$ above $\approx 10^5$ K. Thus in this model the mechanism that Wentzel (1974) has suggested to heat the the arch may trigger the flare. An alternative to this possibility is the long-wavelength ($\approx 10^5$ km) photospheric horizontal waves observed by Tanaka (1972) prior to flares. Mullen (1973) has calculated the energy flux associated with these oscillations, assuming they exist, and finds an energy flux $\mathscr{E}_{flux} \approx 2 \times 10^{10}$ ergs cm^{-2} s^{-1}. Using the observed flaring-

arch length of $\approx 5 \times 10^8$ cm, the possible maximum total power that can be transmitted to an arch is ≈ 40 ergs cm^{-3} s^{-1}, which is of the same order as the radiation losses if $n \approx 10^{12}$ cm^{-3}. A density less than 10^{12} cm^{-3} would lead to a heating of the arch, *especially at the outer boundary.*

This wave energy input could occur in the following way. Assume that these photospheric waves modulate the tension of the magnetic field in the arch. If the modulating period of the photospheric waves is T, and the natural frequency of the arch is Ω, and they together satisfy the condition

$$\Omega T = n\pi \quad (n = 1, 2, 3, \ldots), \tag{5.4}$$

then the photospheric oscillations can result in an amplification of the natural modes of the arch by parametric excitation (Minorvsky, 1962). In general one natural mode of the arch will be the Alfvén mode, whose amplitude can be increased through energy input by the photospheric pump. Since $T = 2\pi/\omega$ and $\Omega = k_\parallel v_A$, we have from Equation (5.4) $\omega = 2k_\parallel v_A/n$. Assuming higher frequency harmonics of the photospheric waves exist, we can write $\omega = \omega_0 m$, $m = 1$ corresponding to the fundamental harmonic. Then $\omega = 2k_\parallel v_A/mn$.

In general, v_A is large for an arch and is about 10^7 or 10^8 cm s^{-1}. Since the waves reported by Tanaka (1972) had a period of ≈ 300 s, we find $\omega_0 \approx 2 \times 10^{-2}$, it follows that the excited Alfvén waves correspond to very long wavelengths parallel to **B**, or the pump waves correspond to very high harmonics, and/or a combination of these possibilities. With the excitation of these Alfvén waves, we can then invoke the mechanisms discussed by Wentzel (1974) for decay of Alvén waves into magnetosonic waves.

In the derivation of the superheating instability, no allowance was made for the coronal heating mechanism. This was neglected simply because the coronal heating mechanism is poorly understood and its inclusion during the derivation would only complicate matters. However *the coronal heating will act as a driving term* if (defining the coronal heating by the function $C(T)$) $\mathrm{d}C/\mathrm{d}T > 0$; i.e., *the coronal heating can actually excite the superheating instability*, particularly if the electrons are preferentially heated over the ions.

Unlike laboratory pinches, arches in the solar atmosphere have a cold core and a hot sheath (Foukal, 1975). We should therefore expect the superheating and rippling modes to be most easily excited within or near this sheath. This should occur for two reasons: first, the density will be lower there and more susceptible to thermal instability; second, the resistivity gradient will be negative as one moves toward the hot sheath, which means the current density will have a maximum in the sheath. such a circumstance is highly unstable to the double tearing mode (Furth *et al.*, 1973), as we will soon discuss.

The formation of this peaked current profile will compete with mechanisms which result in current penetration. The first competing mechanism to be considered is that of normal thermal conduction, perpendicular to the field lines. Earlier we ignored conduction perpendicular to **B**. We were justified then

because, as noted above, arches are typically observed to have hot sheaths; hence, the thermal conductivity would be inward and will only enhance the superheating instability initially. However, as the temperature gradient builds due to the increased joule heating, the increased temperature gradient could stop the growth of current due to increased conduction out of region of instability and into the cooler core. During the rise of j_T the electrons and ions are not very well coupled by collisions, particularly in the low-density sheath, where the collision frequency is further reduced. Hence the only means by which heat can be conducted inward is by electron conduction, the ions being no longer well coupled to the electrons. We therefore need to compare the joule heating terms with the electron thermal conduction perpendicular to **B**.

Using the results of McBride *et al.* (1975) for a similar situation, we find $\beta_p^2 > (R/a)^2$, where $\beta_p = (B_p^2/8\pi nkT_e)^{-1}$. If this condition is satisfied, thermal conduction will stop the current runaway. Since normally $\beta_p < 1$ in the solar atmosphere, and since $R/a > 1$ for an arch, thermal conduction is not expected to inhibit the growth of the current sheath by the resistive instabilities discussed.

The other penetration mechanism of importance is the low frequency electron-temperature-gradient drift wave instability, which is important when the temperature profile is the inverse of the density profile (Kadomtsev, 1965; Lui *et al.*, 1972). This mode requires the magnetic shear to be sufficiently weak so as to not damp the mode. The condition for instability is expressed as

$$\left(1+\frac{T_i}{T_e}\right)\left(\frac{L_n}{L_s}\right)^{3/2} < \left[-\frac{L_n}{2L_T}+\left(1+\frac{T_e}{T_i}\right)\frac{k_y^2\rho_i^2}{\sqrt{2}}\left(\frac{m_e}{m_i}\right)^{1/2}\ln\left[\frac{m_i}{m_e}\left(\frac{L_n}{L_s}\right)^{1/2}\right]\right], \tag{5.5}$$

where $L_s \approx 2.39\times 10^9 B_p/j_T$, $L_n \approx (n^{-1}\,\mathrm{d}n/\mathrm{d}r)^{-1}$, and $L_T \approx (T_e^{-1}\,\mathrm{d}T_e/\mathrm{d}r)^{-1}$.

To see if the condition for this mode can be satisfied, we assume the pressure profile is force free, i.e., $|L_T| \approx |L_n| \approx r_0$. Equation (5.5) shows that when $|L_s| \gtrsim |L_n|$, the condition is most easily satisfied. Taking $L_s \approx L_n \approx r_0$, we find

$$5.23\left(1+\frac{T_i}{T_e}\right) < \left[\tfrac{1}{2}+\left(1+\frac{T_e}{T_i}\right)\frac{k_y^2\rho_i^2}{\sqrt{2}}\right]. \tag{5.6}$$

Since $\rho \approx 0.81$ cm and $k_y \approx m/r_0$, we find $\rho_i^2 k_y^2 \ll 1$, and Equation (5.6) reduces to $5.23(1+T_i/T_e) < \frac{1}{2}$. However, since $T_e/T_i \gg 1$ by assumption, this relation can never be satisfied, and it appears that unless the shear length is such that $L_s \gg L_n$ in an arch, this condition is almost impossible to satisfy.

Apparently once the current runaway begins, there is nothing to stop the buildup of current in the hot sheath of an arch except MHD kink and resistive kink instabilities or current-driven electrostatic instabilities. Using the condition $j_T R/cB_T < 1$ and the threshold conditions for current-driven electrostatic modes it is easy to show that MHD kink and resistive kink instabilities have a much lower instability threshold than current-driven electrostatic instabilities. Thus we expect

the MHD kink and resistive kink instabilities to occur in the arch long before the bulk current could ever become electrostatically unstable. These macromodes will then flatten the current profile by releasing the energy in the form of a flare.

The peaked current profile, caused by the mechanisms discussed above, is particularly unstable to macromodes, because $\mathbf{k} \cdot \mathbf{B} = 0$ can vanish on either side of the peak. This is because $q \propto r/B_p$ is a double-valued function of r. This can be seen using the skin-current-layer model (Furth *et al.*, 1973) $b = x^3/(1+x^2)^2$, where $b = B_p(r)/|B|$, $x = r/r_0$, and r_0 corresponds to where $x = 1$ and measures the current shell width.

A more dramatic form of the tearing mode, in which mulitple tearing should occur, follows from the force-free Bessel-function model and the helically symmetric three-dimensional solutions discussed by Spicer (1976a). To see this, we first note $j(r) = \alpha(r)B(r)$. In equilibrium j_T is proportional to $B_T = B_0 J_0(\alpha r)$; hence $j_T = (c\alpha/4\pi)B_0 J_0(\alpha r)$. Thus j_T will be alternately positive and negative, permitting multiple tearing on either side of the local current peaks and wells. This type of current distribution is particularly susceptible to overlapping resonances because of the neighboring resonant surfaces where $\mathbf{k} \cdot \mathbf{B} = 0$. Such a situation would easily occur in arches with return currents, since the currents will change sign at various minor radii.

5.3. Site of Initial Current Buildup

We have so far argued that a sequence of resistive instabilities will occur in the hot sheath of current-carrying arches. We would also like to consider where along the arch the growth of these instabilities will be most rapid and thereby locate the probable site of the initial current buildup. To do this, we make the reasonable assumption that the arch has a transition zone within each leg much like the ambient atmosphere in which the arch is embedded. Where the temperature minima occur within each leg of the arch need not be the same as the altitude of the temperature minimum in the ambient atmosphere (due to more concentrated wave heating within each leg). However we will further assume that these minima occur within the arch at altitudes similar to the altitude of the temperature minimum in the ambient atmosphere. These assumptions necessarily imply that a steep temperature gradient exists within each leg of the arch around each minimum. Such a gradient alters one of the assumptions that was made in deriving the dispersion relation for the superheating instability: the temperature was not a function of height. When this assumption is relaxed, three new terms appear in the dispersion relation for the superheating instability which now has the form

$$\omega(z) = -i\chi_{\parallel}^0 k_{\parallel}^2 - i\chi_{\perp}^0 k_{\perp}^2 - \frac{\partial \chi_{\parallel}^0 k_{\parallel}}{\partial z} + i\frac{\partial \chi_{\parallel}^0}{\partial T_0}\frac{\partial^2 T_0}{\partial z^2} - \frac{\partial \chi_{\parallel}^0 k_{\parallel}}{\partial T_0}\frac{\partial T_0}{\partial z} - \\ - i\nu_r + i\nu_q \frac{(k_{\perp}^2 - k_{\parallel}^2)}{k^2}. \quad (5.7)$$

In the limit $k_{\parallel} \to 0$ a term remains in (5.7) which is proportional to $\partial^2 T_0/\partial z^2$ and acts as a driving term for the instability if $\partial^2 T_0/\partial z^2 > 0$. Physically this it to be expected. As an electron that is driven by an electric field moves through a region where both the temperature and temperature gradient are increasing, the electron's mean free path is likewise increased, and the electric field can act on the electron for longer intervals of time between collisions. The greater $\partial^2 T_0/\partial z^2$, the greater the effective runaway. Hence, because $\partial^2 T_0/\partial z^2$ is positive for a current with a drift velocity moving in the same direction at T_0 is increasing, and because $\partial^2 T_0/\partial z^2$ is greatest in the transition zone, the superheating instability should be expected to have its greatest rate of growth there. Although we have not treated the density decrease with height in the arch, this decrease in n will have an effect similar to an increase in T_0. From this we conclude that the origin of the initial preflare heating, by the mechanisms discussed, is in the region along the arch where the transition zone occurs. This may be along the leg of the arch or at its top, depending on the height of the arch and the heating mechanism causing the temperature gradient. *Again it appears within the context of this model that the coronal heating mechanism may be related to the origin of the flare.*

Other mechanisms that can lead to this form of current runaway are a gradual twisting of the field, a gradual shearing of the field by lateral foot motion, or a transient EMF along **B** of unknown origin. The first two occur because the current is steadily increasing and at some stage will start to run away by the combination of resistive instabilities and the external current driver. We expect shearing to be important as a precusor effect, because large shear will actually increase the likelihood of the tearing instability. The effect of a transient EMF on $\mathbf{j}_{\parallel}$ is obvious.

A modification of the basic superheating instability could occur, if there were an electron beam stably trapped in the arch, since this beam could lead to an increase in bulk resistivity in the presence of an electrostatically stable current by the mechanism of Papadopoulos and Coffey (1974a, b). Hence, since this resistivity is a bulk resistivity, the joule heating would increase in its presence. This increase in joule heating would then lead to more electron runaway, which then feeds the beam that generates the anomalous resistivity. If this proposed mechanism were to occur, a self-sustaining nonlinear feedback mechanism between current and beam could lead to the current buildup desired. Earlier we found that this mechanism increased the resistivity for the adopted parameters by 10^2. In addition it was noted in Section 3 that this mechanism was most effective in increasing the resistivity in regions of lower density, which in an arch would correspond to the arch apex and within the hot sheath. Thus the mechanism fits into the sequence of instabilities discussed earlier, where the resistivity was assumed classical. The increase in η by 10^2 will lower the required j_F by 10 for the onset of the superheating instability.

Since this mechanism requires a beam of electrons, we must find a source for such a beam. The most obvious and most reasonable source of such a beam would be the runaway high-energy tail of the electron current distribution function. The

number density in the tail of a Maxwellian is obtained by integrating the ambient Maxwellian from v_0, to infinity, obtaining

$$\frac{n_T}{n} = \frac{2}{\sqrt{2\pi}} \frac{\exp\left(-\frac{v_0^2}{2v_{T_e}^2}\right)}{\left(\frac{v_0}{v_{T_e}}\right)}. \tag{5.8}$$

Taking $v_0 \approx 3v_{T_e}$, we obtain $n_T/n \approx 2.95 \times 10^{-3}$. Since $n \approx 10^{12}\ \mathrm{cm}^{-3}$, we find $n_T \approx 2.95 \times 10^{9}\ \mathrm{cm}^{-3}$, which is 10^3 times larger than the number of electrons required to form the beam as calculated earlier from Equation (3.19). Hence, only 10^3 of the tail electrons need to run away to form the beam.

5.4. Location of Initial Instability in the Arch

Although we have examined where the most probable initial current buildup should occur, it does not necessarily follow that the flare instability should start there. Indeed as shown Spicer (1976a), the safety factor will be a minimum at the apex of the arch, assuming the toroidal component of **B** is the same in both legs. In general however B_T in one leg will not necessarily be the same as in the other. Thus, it follows that q will have its minimum, as a function of the toroidal coordinate, at different locations for different arches. However, since j_T will have its greatest growth in the transition zone of the arch, one should expect the instability to start somewhere between this region and the apex of the arch, assuming that the transition zone does not coincide with the top of the arch and that B_T is the same in both legs of the arch. For any other set of circumstances the picture becomes more complicated, and an accurate prediction can be made only when the physical details of arches become known.

6. Phenomenological Aspects of the Flare Model

This section will be devoted primarily to examining the flare model in various situations which are believed to occur on occasion.

However, before proceeding we emphasize that any magnetic topology which contains a current and has magnetic shear should be susceptible to just about every instability we have discussed. This should include X-ray bright points, filaments, GRF events, and loops in general. This will help in understanding the relationship between flares and filaments.

6.1. Expected Observational Characteristics of the Model

As seen in Section 5, our flare model is intrinsically associated with preflare effects, which dictates whether a flare will or will not occur. What then is the expected phenomenological behavior of this model? Essentially two types of arches are to be considered: the emerging arch and the preexisting arch. A single

emerging arch is difficult to treat. Hence, while we consider them as potential candidates for flaring, we will confine our discussion to preexisting arches with the exception of an emerging arch interacting with a preexisting filament or arch similar to the Canfield *et al.* (1974) model.

Preexisting arches will flare if one can alter the magnetic shear sufficiently to trigger the MHD kink and resistive kink modes. In *addition the magnitude of this shear will determine whether the flare will exhibit weak or strong impulsive behavior* in the form of nonlinear overlapping resonances and global kinks. Further, we have found there exists basically two means by which the shear of the field can be altered, namely a steeping of the current-density profile by either transport mechanisms or transient phenomena. Alteration of the current-density profile by transport mechanisms was shown to be closely related to mechanisms that are believed to heat the corona. Hence we expect this type of mechanism to result from a preheating of the arch, i.e., the flux of waves believed to heat the corona must be increasing in the arch, thereby altering the current-density profile by the resistive modes discussed. Logically there is no reason why one arch should be singled out from other arches in an active region during this increase in wave flux. Thus we should expect preheating in all arches. If this is the case, why should a few arches flare and not all arches in the active region? The answer is that preheating, and the subsequent current density profile steepening, is only a part of a sequence of events which ultimately leads to a flare. The preheating prepares the arch for flaring, and the transient motions provide the final push necessary to start the flare. This occurs because the current steepening will be balanced by the weak dissipation of the current, when the shear becomes steep enough to excite the tearing mode, so that the system will evolve into a state of marginal stability. During this period an increase in heating will occur, above that due to the preheating. In addition impulsive behavior may occur due to weak kink and resistive kink modes. The actual onset of the flare will occur when either an external transient provides the push or the arch itself nonlinearly evolves into a strong global kink. The global kink will result in the effects discussed in Section 4. Some possible transient effects that may push the arch into instability are illustrated in Figure 8.

With what has been said, what should be observed? Obviously a general preheating of the arches in the active region should be observed. This preheating should be particularly strong in the transition zone, because most of the wave flux will dissipate there. The arch should appear to brighten substantially, particularly the plasma boundary, which should sharpen with time; this occurring over a period of hours or minutes, as shown in Section 5. If the preheating is maintained for the proper interval, an extended burst and possibly weak IEBs should appear. This period corresponds to the marginal state just discussed. Two things can now occur: the arch may remain in a marginal state until the heating source is shut off and the current profile relaxes or the arch may flare, being pushed into flaring by some transient phenomena, e.g., emerging magnetic flux.

What occurs during the actual flare is difficult to state precisely, *since the evolution of each flare is highly nonlinear and thus unique.* However we can heuristically discuss the general sequence of events. If the flare is thermal, in the extreme sense discussed in Section 4, very little dynamic behavior will occur as far as the arch is concerned. *The volume of energy release will generally be small compared to the total-volume* field energy *of the arch and will be situated in the leg of the arch* where the current flows parallel to the temperature gradient. The localized energy release will cause heat to diffuse out of the heated region, increasing the volume of apparent instability. Hence, *from an observational point of view, there will be a small core or cores of hot plasma surrounded by decreasing temperature gradients;* i.e., *the flaring arch will have a multithermal structure.* Since the rate of energy release is slower, we expect any shock waves excited to be weak, if they are excited at all. We expect these flares to occur in arches with larger volumes or densities than those in which the impulsive flares which release an equivalent amount of energy occur.

The nonthermal impulsive flare is similar to the thermal flare, except the rate of energy release is much greater and strong resonant overlap can occur as well as global kink modes. We can then expect strong blast waves and strong bursts of impulsively heated and accelerated particles. Figure 10 illustrates the basic sequence of events *if the flare is excited by external heating mechanisms.*

Recently a flare model based on *emerging arches* interacting with preexisting magnetic structures has been advanced (Canfield *et al.*, 1974). This model was advanced because of the strong correlation between emerging flux and filament flares (Rust and Roy, 1974; Zirin, 1974) and the subsequent activation of filaments (Rust *et al.*, 1975). This type of flare is different, e.g., from that observed by Petrasso *et al.* (1975) in which a preexisting arch itself preheated and then flared in a manner similar to that just discussed theoretically. Because of this difference in flare types, it is of interest to examine whether the model advanced here can also satisfy these interesting observations.

The mechanism invoked by Canfield *et al.* (1974) to explain the energy release of the flare was that at the interface between the interacting emerging arch and preexisting filament (or similar configuration) a current sheet is formed and when the current density within the sheet exceeds a critical value, rapid magnetic reconnection takes place producing the desired flare. Let us ask 'what would occur if a *current carrying arch*, as discussed throughout this paper, were to interact with a preexisting filament or similar configuration'? Granted a current sheet interface may form, as emphasized by Canfield *et al.* (1974). However, more importantly if the pressure exerted between the two magnetic configurations is sufficient to cause the current density within the sheet to grow, as required by Canfield *et al.* (1974), it is also sufficient to compress and distort the nested magnetic surfaces within the emerging current carrying arch and within the filament (Figure 11). This compression would eventually result in significant reconnection *within the emerging arch itself and the filament,* if the filament

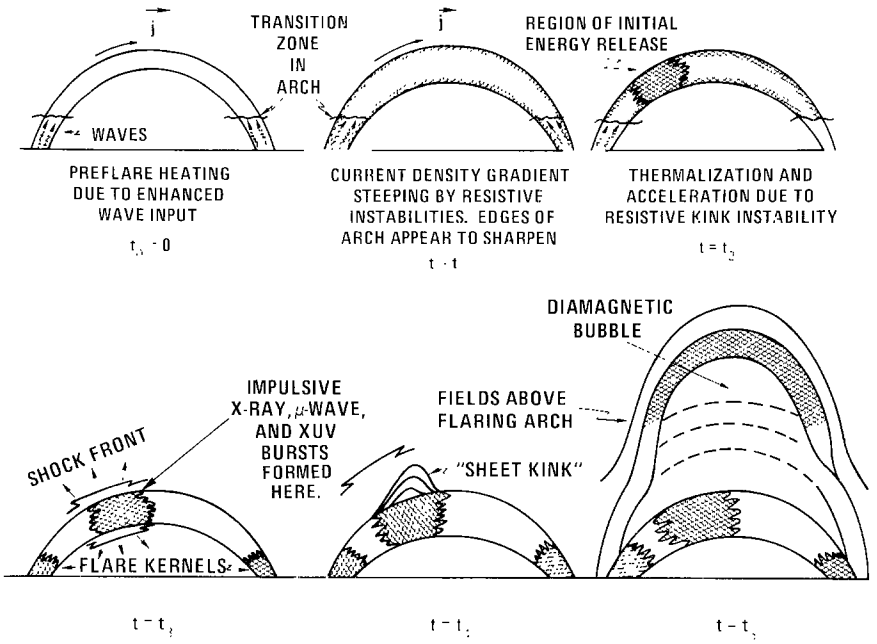

Fig. 10. Emerging current carrying arch, interacting with a pre-existing magnetic structure.

possesses a sheared magnetic field. The reconnection within the arch itself would explain the energy release of the flare rather than the sheet formed (if ever formed) at the interface between the configurations.

Obviously the strengths of this model over that envisaged by Canfield *et al.* (1974) is that a sizable volume within which reconnection takes place is obviously preferred to an extremely thin reconnecting sheet at the interface between the two configurations. In addition, there is no absolute need for turbulent resistivity, since the volume in which reconnection is occurring is significantly increased over that of one sheet. A further point worth noting is that when reconnection rate is determined by the fluid velocity resulting from the pressure at the interface the tearing mode may evolve nonlinearly into a faster Petschek type reconnection (a Petschek box at every neutral point, Kaw, 1976; Spicer, 1976b). Because of this the magnetic islands formed during the tearing mode process will expand substantially beyond that predicted by linear theory (Kaw, 1976; Spicer, 1976b, 1977b). Under these circumstances interaction of neighboring reconnecting layers becomes more likely (Spicer, 1976a) and the rate of magnetic field thermalization per unit volume can increase substantially (Spicer, 1976b) producing the nonthermal effects common to flares.

If one who is familiar with the Canfield *et al.* (1974) model can ignore the differences in energy release mechanisms advanced by Canfield *et al.* and that presented here he should realize that the resulting models are essentially the same and therefore have similar phenomenological consequences. Hence, the principal

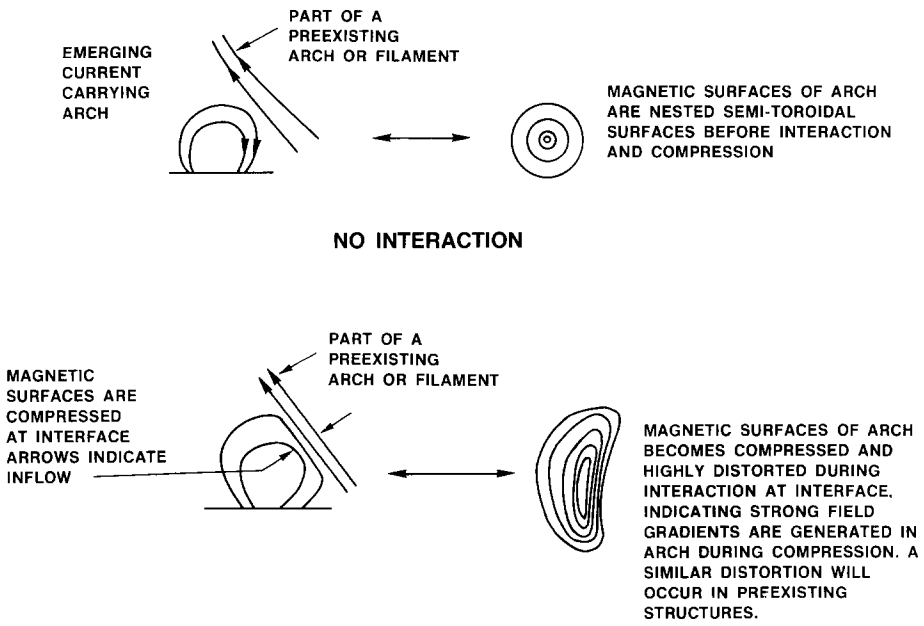

Fig. 11. Example of events that can lead to a flare.

difference is the volume and rates of energy release and the type of emerging arches. Or to put it otherwise the energy release mechanism presented here can do the same job as the simple sheet and can do it better. In addition, we find that incorporating emerging flux into the model presents no problem if the situation envisaged by Canfield *et al.* (1974) is physically the situation (e.g., an alternate possibility would be a simple current carrying arch emerging and flaring but not directly interacting with the filament except through the strong hydrodynamic effects produced by the flare). Thus we can conclude that we can explain flares occurring in pre-existing arches, as described by Petrasso *et al.* (1975) and those described by Rust and Roy (1974) and Zirin (1974) using a simple arch.

7. Discussion and Conclusions

In the development of this model we have used the observational fact that the magnetic topology of a flare appears as an arch. In addition we have assumed that a toroidal current exists in the arch. With this, we have examined the physical consequences of the assumption and how it relates to the solar flare. We have found that the consequences are many and that the model can explain many of the observations obtained from Skylab, as well as previous observations. The assumption of the existence of such a current has led, quite naturally, to a flare

model that has explanations for many varied phenomena, which include:

- The role of preflare heating.
- The small volume of energy release within the arch in comparison to the total arch volume.
- The integrity generally maintained by the arch.
- The difference between thermal and nonthermal flares.
- Kinking arches.
- A close relationship that may exist between flare instabilities and filament instabilities if the filaments contain currents.

We predict that:

- The nonthermal flare, large or small energy release, will generally come from low altitude arches.
- Impulsive bursts are a result of nonthermal heating and strong disruptions of the plasma.
- The thermal flare will come from larger arches, unless the plasma density is very large and invalidates Equation (4.1), even in the presence of large fields and field gradients.
- The rate of energy release decreases with increasing volume.
- Type III bursts either escape from arches by drift mechanisms and/or are caused by sheet kinks.
- Shock waves may excite multiple arches to flaring by a domino effect.
- Energy is stored mainly in the form of currents generated beneath the visible photosphere, and the total stored energy is probably much greater than the actual energy released during a flare.
- The faster the flare rise time the more nonthermal the flare.
- High-altitude arches with weak field gradients will have large-diameter magnetic islands, and low-altitude arches with strong field gradients will have small-diameter magnetic islands, with both high and low arches having the appearance of being stranded like a rope.

Some of these explanations are heuristic, but this is by necessity and not by choice. For the theorist to develop a more quantitative model will require high instrumental resolution, which will not become available in the foreseeable future. However the theorist must complement the observer regardless of the observer's instrumental weaknesses. Hence the theorist must, within his ability, help guide the observer in his observations, and for him to do so requires a model which is reasonably complete and which can be tested. If tests prove positive, this model or a more successful model can then be quantitatively improved, such as by a numerical modeling. However at present only particular features of this model need to be studied in more detail, e.g., overlapping resonances and the degree of enhanced reconnection, or the phenomenological release of the equivalent of a flare energy into a model solar atmosphere, using realistic numerical techniques. In this way progress can be made theoretically, and simultaneously other problem areas can be defined.

It is hoped that this model, whether correct or incorrect, will act as a catalyst for others and make the development of more realistic theoretical models of flares a reality. In addition it is hoped that the observer will give it a chance and compare theory with observations carefully, being cautious not to confuse flare manifestations with the actual event.

Acknowledgements

The author thanks Profs. D. A. Tidman and C. S. Liu and Drs D. Book and E. Toton for many fruitful conversations during various stages of this research. The author is also grateful to Drs K. G. Widing and G. Doschek for interesting discussions on flare observations and Dr G. Brueckner for introducing him to the solar flare problem.

Final thanks to Drs H. Friedman and R. Tousey for supporting this research at NRL.

References

Alfvén, H. and Carlquist, P.: 1967, *Solar Phys.* **1,** 220.
Brown, J.: 1974, in G. Newkirk, Jr. (ed.), 'Coronal Disturbances', *IAU Symp.* **57,** 395.
Brueckner, G.: 1976, *Phil. Trans. Royal. Soc. (London)* **A281,** 1304.
Brueckner, G. E., Patterson, N. P., and Scherrer, V. E.: 1976, *Solar Phys.* **47,** 127.
Canfield, R. C., Priest, E. R., and Rust, D. M.: 1974, in *Flare Related Magnetic Field Dynamics*, HAO, Boulder, Colo.
Cheng, C. C. and Widing, K.: 1975, *Astrophys. J.* **201,** 735.
Finn, J. M.: 1975, AEC Res. Dev. Rep. Matt-1137, Princeton Univ.
Finn, J. M. and Kaw, P. K.: 1976, AEC Res. Dev. Rep. Matt-1220, Princeton Univ.
Foukal, P.: 1975, *Solar Phys.* **43,** 327.
Furth, H. P., Rutherford, P. H., and Selberg, H.: 1973, *Phys. Fluids* **16,** 1054.
Furth, H. P., Killeen, J., and Rosenbluth, M. N.: 1963, *Phys. Fluids* **6,** 459.
Gibson, E. G.: 1977, *Solar Phys.* **53,** 123.
Glasstone, S. and Lovberg, R. H.: 1960, Controlled Thermonuclear Reactions, Van Nostrand, Princeton, N.J.
Guzdar, P. N., Sen, A., and Kaw, P. K.: 1975, *Nucl. Fusion* **15,** 1007.
Jackson, J. D.: 1962, *Classical Electrodynamics*, Wiley, New York.
Janssens, T. J., White, K. P., III, and Broussard, R. M.: 1973, *Solar Phys.* **31,** 207.
Kadomtsev, B. B.: 1976, ERDA Translation, Matt-Trans-119.
Kadomtsev, B. B.: 1965, *Plasma Turbulence*, Academic Press, New York.
Kadomtsev, B. B. and Pogutse, O. P.: 1970 in M. A. Leontovich (ed.), *Reviews of Plasma Physics* **5,** Consultants Bureau, New York.
Kadomtsev, B. B.: 1966, in M. A. Leontovich (ed.), *Reviews of Plasma Physics* **2,** p. 153, Consultants Bureau, New York.
Kahler, S. W., Krieger, A. S., and Vaiana, G. S.: 1975, *Astrophys. J. Letters* **199,** L57.
Kaw, P. K.: 1976, ERDA Res. Dev. Rep. Matt-1264, Princeton Univ.
Krall, N. A. and Trivelpiece, A. W.: 1973, *Principles of Plasma Physics*, McGraw-Hill, New York.
Liu, C. S.: 1971, *Phys. Rev. Letters* **27,** 1637.
Liu, C. S., Rosenbluth, M. N., and Horton, C. W.: 1972, *Phys. Rev. Letters* **29,** 1489.
McBride, J. B., Klein, H. H., Byrne, R. N., and Krall, N. A.: 1975, *Nucl. Fusion* **15,** 393.
McWhirter, R. W. P., Thoneman, P. C., and Wilson, R.: 1975, *Astron. Astrophys.* **40,** 63.
Moreton, G. and Severny, A.: 1968, *Solar Phys.* **3,** 282.

Mullen, D. J.: 1973, *Astrophys. J.* **185,** 353.
Papadopoulos, K. and Coffey, T.: 1974a, *J. Geophys. Res.* **79,** 674.
Papadopoulos, K. and Coffey, T.: 1974b, *J. Geophys. Res.* **79,** 1558.
Papadopoulos, K.: 1975, private communication.
Parker, E. N.: 1955, *Astrophys. J.* **122,** 293.
Parker, E. N.: 1973, *Astrophys. J.* **180,** 247.
Petrasso, R. D., Kahler, S. W., Kreiger, A. S., Silk, J. K., and Vaiana, G. S.: 1975, *Astrophys. J. Letters* **199,** L127.
Purcell, J. D. and Widing, K.: 1971, *Astrophys. Letters* **179,** 239.
Rust, D. M. and Roy, J. R.: 1974, AFCRL No. 474.
Rust, D. M., Nakagawa, Y., and Neupert, W.: 1975, *Solar Phys.* **41,** 397.
Sverny, A.: 1965, *Astron. Zh.* **42,** 217.
Sheeley, N.: 1976, *Solar Phys.* **47,** 173.
Smith, D. F. and Priest, E. R.: 1972, *Astrophys. J.* **176,** 487.
Solovev, L. S.: 1971, *Soviet Atomic Energy* **30,** 14.
Spicer, D. S., Cheng, C. C., Widing, K., and Tousey, R.: 1974, paper presented at the 2nd European Conference on Cosmic Plasma Physics, Culham, England.
Spicer, D. S.: 1975, *Bull. Am. Astron. Soc.* **7,** 352.
Spicer, D. S.: 1976a, NRL Formal Report 8036.
Spicer, D. S.: 1976b, NRL Memo 3465.
Spicer, D. S.: 1977a, *Solar Phys.* **51,** 431.
Spicer, D. S.: 1977b, *Solar Phys.* **53,** 249.
Spitzer, L.: 1967, *Physics of Fully Ionized Gases*, Interscience, New York.
Sturrock, P. A.: 1966, *Nature* **211,** 695.
Sturrock, P. A.: 1968, in K. O. Kiepenheuer (ed.), 'Structure and Development of Solar Active Regions', *IAU Symp.* **35,** 471.
Sturrock, P. A.: 1972, *Solar Phys.* **23,** 438.
Sturrock, P. A.: 1973, in R. Ramaty and R. G. Stone (eds.), *Proc. Symposium on High Energy Phenomena on the Sun*, NASA Goddard Space Flight Center, p.3.
Syrovatskii, S. I.: 1966, *Soviet Astron.* **10,** 270.
Tanaka, K.: 1972, Big Bear Solar Observatory preprint, unpublished.
Tidman, D. A. and Krall, N. A.: 1971, *Shock Waves in Collisionless Plasmas*, Wiley-Interscience, New York.
Tidman, D. A. and Stamper, J. A.: 1973, *Appl. Phys. Letters* **22,** 498.
Title, A. M. and Andelin, J. P.: 1971, in R. Howard (ed.), 'Solar Magnetic Fields', *IAU Symp.* **43,** 298.
Von Goeler, S., Stodiek, W., and Sauthoff, N.: 1975, Matt-1058, Princeton, N.J.
Vorpahl, J. A., Gibson, E. G., Landecker, P. B., McKenzie, D. L., and Underwood, J. H.: 1975, *Solar Phys.* **45,** 199.
Wentzel, D. G.: 1974, *Solar Phys.* **39,** 129.
Widing, K.: 1974a, in S. R. Kane (ed.), 'Solar Gamma-, X-, and EUV Radiation', *IAU Symp.* **68,** 153.
Widing, K.: 1974b, *Astrophys. J. Letters* **197,** L33.
Widing, K. and Cheng, C. C.: 1975, *Astrophys. J. Letters* **194,** L155.
Widing, K. and Dere, K.: 1977, to appear in *Solar Phys.*
Zirin, H.: 1974, *Vistas Astron.* **16,** 1.